UNIVERSITÀ DI PARMA
ARCHIVIO DELLA RICERCA

University of Parma Research Repository

The Messinian Salinity Crisis Between Italy and Albania: The Peri-Adriatic Depression and Southern Adriatic Basin Records

This is the peer reviewd version of the followng article:

Original
The Messinian Salinity Crisis Between Italy and Albania: The Peri-Adriatic Depression and Southern Adriatic Basin Records / Bigi, D., Lugli, S., Manzi, V., Roveri, M., Milushi, I.. - In: BASIN RESEARCH. - ISSN 0950-091X. - 38:2(2026). [10.1111/bre.70096]

Availability:
This version is available at: 11381/3074750 since: 2026-09-21T08:41:34Z

Publisher:
John Wiley and Sons Inc

Published
DOI:10.1111/bre.70096

Terms of use:

Anyone can freely access the full text of works made available as "Open Access". Works made available

Publisher copyright

note finali coverpage

(Article begins on next page)

13 November 2026

Basin Research

WILEY | IAS

RESEARCH ARTICLE OPEN ACCESS

The Messinian Salinity Crisis Between Italy and Albania: The Peri-Adriatic Depression and Southern Adriatic Basin Records

Bigi Diego[1] | Lugli Stefano[2] | Manzi Vinicio[1] | Roveri Marco[1] | Milushi Ibrahim[3]

[1]Dipartimento di Scienze Chimiche, Della Vita e Della Sostenibilit'a Ambientale, University of Parma, Parma, Italy | [2]Dipartimento di Scienze Chimiche e Geologiche, Università di Modena e Reggio Emilia, Modena, Italy | [3]Institute of Geosciences, Polytechnic University of Tirana, Tirana, Albania

Correspondence: Manzi Vinicio (vinicio.manzi@unipr.it)

Received: 17 June 2025 | **Revised:** 12 February 2026 | **Accepted:** 20 February 2026

ABSTRACT

We reconstructed the geological evolution of the Albanides during the Messinian salinity crisis (MSC), based on the integration of outcrop and subsurface data from both onshore (peri-Adriatic depression, Albania) and offshore (Southern Adriatic Basin) settings. The lowermost MSC deposit consists of primary bottom-grown gypsum accumulated in marginal basins (Rubjekë, Durres inland; Guri i Cifutit, Vlora) of the peri-Adriatic depression. Facies analysis and Sr. isotope signature allow correlating these deposits with the Primary Lower Gypsum unit (PLG). This unit is truncated on top by an erosional surface that can be correlated in deeper settings (Currilla, Durres coast; Kavaje) with a sharp surface separating evaporite-free, organic-rich, and barren shales below from a clastic evaporite unit above. The unconformity can be regarded as the Messinian Erosional Surface and the clastic evaporites as the local expression of the Resedimented Lower Gypsum (RLG). Seismic and geophysical logs allow following this unit offshore in a WNW direction for hundreds of kilometres. While in the marginal settings the PLG are overlain by marine Pliocene deposits, in the deeper settings (Currilla) the RLG unit is overlain by thick terrigenous deposits that can be subdivided into a lower finer-grained barren shale unit followed upward by a rhythmic alternation of conglomerate or sandstone bodies and shales. The uppermost portion of this unit contains a typical Paratethyan hypohaline faunal assemblage yielding a depleted Sr. signature and thus referable to the Lago-mare unit, which records the final stage of the MSC. In turn, these deposits are followed by Zanclean open-marine sediments. These findings are in good agreement with the 3-stage model of the MSC and enable the reconstruction of basin-scale correlations from the thrust-top and foredeep basins of the Albanides and the Apennines, through the Adria foreland.

1 | Introduction

The distribution of the deposits related to the Messinian Salinity Crisis (MSC) in the Apennines and in the Adriatic foredeep is well-known after several studies focused on the evolution of the Apennine foredeep (Iaccarino and Papani 1980; Iaccarino and Salvatorini 1982; Roveri et al. 1998, 2001, 2003, 2008a; Roveri, Flecker, et al. 2014) and the Adriatic foreland (Roveri et al. 2005; Hüsing et al. 2007, 2009; Iaccarino et al. 2008; di Stefano et al. 2010; Manzi et al. 2020). In particular, the large amount of subsurface data from the Adriatic offshore published by the Italian Ministry of Economic Development through the project "Visibility of petroleum Exploration Data in Italy" (ViDEPI), allowed Manzi et al. (2020) to reconstruct the occurrence of Messinian evaporites along the entire Apennine foredeep and foreland. According to the stratigraphic framework proposed by Roveri et al. (1998, 2001, 2003) and subsequent update (CIESM 2008), the MSC unfolded in three stages. During stage 1 the precipitation of the Primary Lower Gypsum (PLG) occurred only in the higher structural contexts, i.e., in the wedge-top and

This is an open access article under the terms of the Creative Commons Attribution License, which permits use, distribution and reproduction in any medium, provided the original work is properly cited.

© 2026 The Author(s). *Basin Research* published by International Association of Sedimentologists and European Association of Geoscientists and Engineers and John Wiley & Sons Ltd.

Highlights

- The Messinian salinity crisis in Albania: outcrops and subsurface data integration.
- Cross-Adriatic correlation of the Albania and Northern Apennines foredeeps.
- Reconstruction of the geological evolution of the Albanides during the Messinian salinity crisis.
- Confirm the validity of the 3-stage model also for the eastern side of the Adriatic Sea.

Adriatic foreland basins (Roveri et al. 2003). The more complete PLG succession is found in the Vena del Gesso wedge-top basin, where up to 16 shale/gypsum precessional-driven cycles have been described (Lugli et al. 2010). Other minor piggy-back basins are found more to the south, in the Marecchia Valley (Gennari et al. 2013), Irpinia (Matano et al. 2005) and Molise (Cosentino et al. 2018). Evaporite deposition took place also in the shallower settings of the Adriatic foreland ramp, where the largest PLG basin of the whole Mediterranean has been recognised (Manzi et al. 2020). The main depocenter is in the Adriatic offshore between the Gargano and Conero highs (Ori et al. 1986; Roveri et al. 2005; Corcagnani 2017), but the primary evaporites extend in a north-west direction below the Po River plain, reaching the subsurface of the Ferrara town (Rossi et al. 2015; Manzi et al. 2020). This unit is commonly incomplete, being truncated at the top by the Messinian erosional surface (MES; Roveri, Flecker, et al. 2014); the boreholes showing the higher number of gypsum cycles are located between the Gargano high and the Gran Sasso massif in Central Italy. The good preservation of the PLG in this area can be explained by the rapid tectonic subsidence produced by the eastward migration of the Apennine thrust front (Manzi et al. 2020). In the more depressed wedge-top basins and in the main foredeep, an interval of organic-rich shale was deposited instead of the primary gypsum (Manzi et al. 2007; Rossi et al. 2015; FBI *sensu* Manzi et al. 2018, 2021). During stage 2, the same foredeep areas largely coincided with the depocenters of the Resedimented Lower Gypsum (RLG), a clastic unit consisting of resedimented gypsum derived from the dismantlement of the PLG unit (Manzi et al. 2005; Roveri et al. 2006; Roveri, Flecker, et al. 2014). Differently from the other southern sectors of the Mediterranean, in the Adriatic foredeep the deposition of halite (stage 2) and Upper Gypsum (stage 3) did not occur. Due to the absence of primary evaporites, the entire succession younger than the PLG (post-5.60 Ma) found above the MES was originally included in the post-evaporitic unit (Roveri et al. 1998, 2001), consisting of a lower p-ev$_1$ unit, including the resedimented evaporites (RLG; stage 2), and an upper p-ev$_2$ unit characterised by coarser-grained deposits related to an increased siliciclastic input starting from 5.42 Ma, which was punctuated by whitish carbonate layers of chemical origin (the "colombacci" sensu Selli 1952, 1954). The post-evaporitic unit is characterised by the occurrence of peculiar hypohaline fossil assemblages (mostly ostracods, molluscs, dinocysts) with Paratethyan affinity, that in the p-ev$_2$ show the higher specific diversity and abundance. Due to the peculiar fossil content pointing to more humid climate conditions, this interval was termed "Lago-mare" (Gignoux 1936; Ruggieri 1967; Andreetto et al. 2021; Roveri et al. 2026).

An important stratigraphic proxy for the MSC is the $^{87}Sr/^{86}Sr$ signature of rocks and fossils that during the interval between the onset of the crisis (5.97 Ma; Manzi et al. 2013) up to the Messinian/Zanclean boundary (5.32 Ma; van Couvering et al. 2000) is characterised by diagnostic excursions. During stages 1 and 2, the Mediterranean experienced a first reduction of the oceanic input (Flecker et al. 2002; Flecker and Ellam 2006; Gladstone et al. 2007; Topper et al. 2011, 2014; Topper and Meijer 2013) reflected by a first detachment from the global ocean values. A second major deviation is associated with stage 3, also characterised by the spread of the Lago-mare hypohaline assemblages. For these reasons, the $^{87}Sr/^{86}Sr$ of evaporite and carbonate allows us to distinguish among stages 1 and 2 (PLG and RLG) and stage 3 (UG); as for the final stage, devoid of evaporites, both micro- (ostracods, foraminifera) and macro-fossils (mollusc shells) may provide useful geochemical data for the identification of the Lago-mare deposits (Roveri et al. 2026).

Despite the remarkable level of knowledge gained for the Apennines and the Western Adriatic offshore, subsurface and outcrop data for the Dinaric side are quite scarce. The MSC-related deposits only crop out in the western side of the Albanides, close to the Southern Adriatic basin coast, as documented by Pashko (1973); Pashko et al. (2017); Pashko and Aliaj (2020); Buli et al. (2001); Prillo and Hasanaj (2002). Nevertheless, only recently has an accurate dating of the onset of the crisis in the type-section (Kavaje) been proposed by Bigi et al. (2024).

The aim of this work is to reconstruct a chronostratigraphic framework for the evolution of the Messinian salinity crisis in the poorly known South Adriatic region through the integration of subsurface (offshore and onshore) and outcrop data. This area provides pivotal implications for the comprehension of the salinity crisis at Mediterranean-scale in the light of the different proposed stratigraphic models.

2 | Geological Setting

The Southern Adriatic Basin (SAB; Figure 1) is the foredeep basin of the west-verging Albanides fold-and-thrust belt and is bordered to the west by the Apulian Platform. The latter is the foreland of both the Apennines and the Albanides (Ricchetti et al. 1988) and consists of Mesozoic shelf carbonates representing a relatively undeformed portion of the passive margin of the Tethys Ocean (Figure 1A,B). The front of the Albanian orogen can be divided into a northern and a southern sector separated by the Vlore-Elbasan tectonic alignment (V-E; Figure 1A,C). These two sectors are clearly distinguishable because they are differently influenced by the Mesozoic palaeogeography (Argnani et al. 1996; Argnani 2013). In the southern sector, the Apulian Platform is involved in deformation (Figure 1A), justifying the high topographic elevation close to the coast and the very limited foredeep basin. In contrast, the northern sector is represented by the Peri-Adriatic Depression (PAD; Figure 1A,C), where the thickness of the Oligocene-Quaternary foredeep clastic infill reaches 8–10 km moving offshore (Argnani et al. 1996; Argnani 2013). The morphology of the area is structurally controlled by gentle folds related to

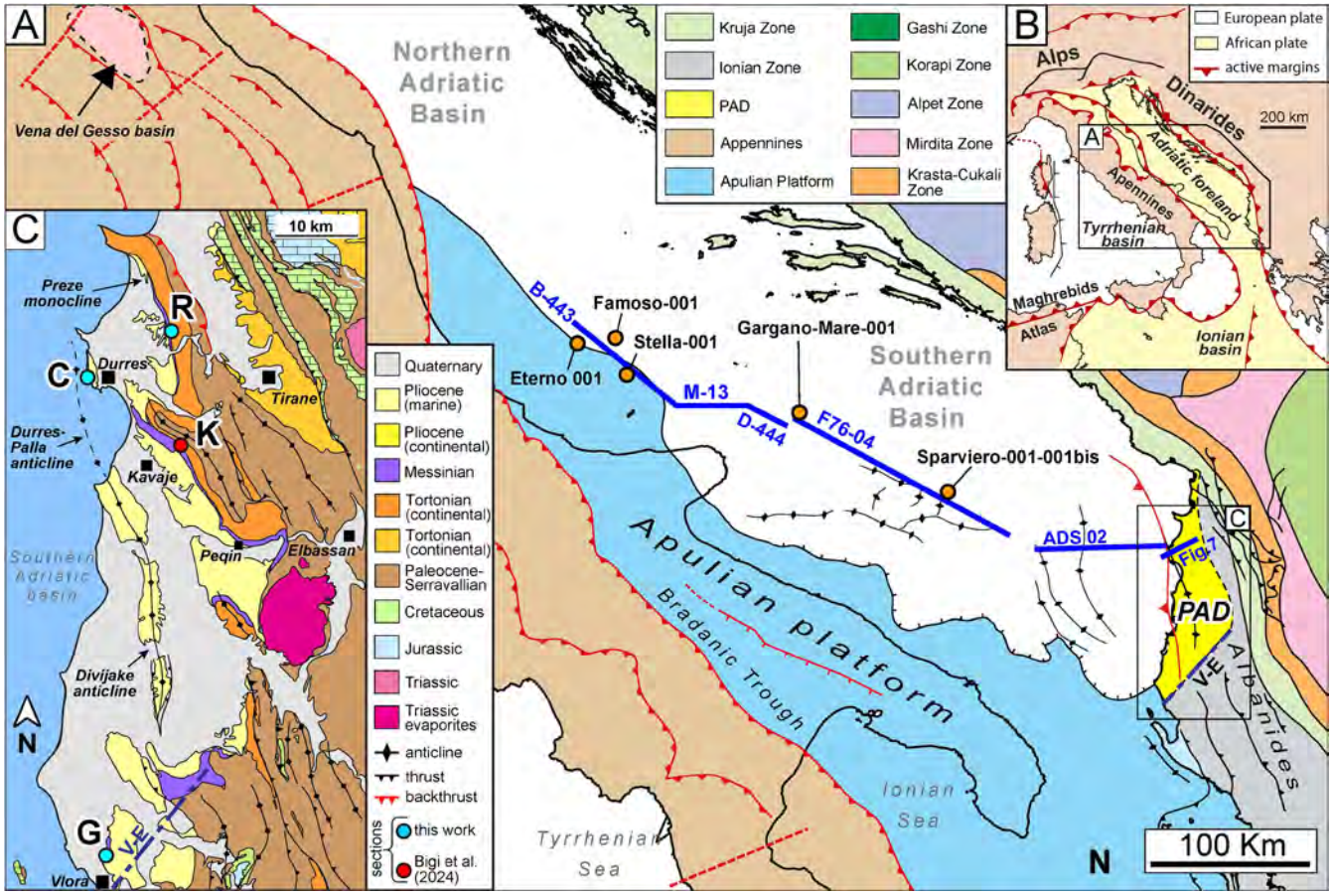


FIGURE 1 | Study area. (A) General geological map of the Adriatic area with location of the seismic lines and boreholes used in this work; (B) geodynamic setting; (C) enlargement and geological map of the Peri-Adriatic Depression (PAD) with location of the study sections (modified from Xhomo et al. 1999; Shërbimi Gjeologjik Shqiptar 2002): Rubjekë (R), Currilla (C) and Guri i Cifutit (G) and the section of Kavaje (K) after Bigi et al. (2024).

active back-thrusts (Muço 1994; Kiratzi and Papazachos 1995; Pondrelli et al. 1995; Vannucci et al. 2004; Sextos et al. 2020).

In this work, in order to extend the investigations recently carried out in the Kavaje (K) section (Figure 1; Bigi et al. 2024) we have studied three stratigraphic sections (Figure 1C): (i) Rubjekë (R), Durres hinterland; (ii) Currilla (C), Durres coast; (iii) Guri i Cifutit (G), Vlora. Moreover, we have used published and partly reviewed subsurface data, including seismic and boreholes data, to correlate the onshore Albanian succession with the sedimentary record of the offshore subsurface Adriatic and of the Apennine chain.

3 | Methods

Three sections, Rubjekë, Currilla, and Guri i Cifutit (Figure 1C), have been investigated with an integrated approach including stratigraphic and sedimentological field work and petrographic, biostratigraphic, and geochemical analyses.

3.1 | Petrographic Analyses

A total of 37 samples (Table S1) have been investigated for microfacies analyses in thin section. Attention was given to gypsum samples to verify the primary, secondary, or clastic origin, the presence of dissolution surfaces and the possible presence of anhydrite. The mollusc and ostracod shells selected for the geochemical analysis were also analysed in thin section to verify their preservation.

3.2 | Biostratigraphic Analyses

A total of 27 samples (Table S2) were selected for micropaleontological analyses at the Micropaleontology Laboratory of the University of Parma. Samples were dried in an oven at 40°C, then soaked in diluted H_2O_2 for a few days and finally washed using a 63 μm mesh sieve. The washed residues were dried and sieved to get both fractions, above and below 125 μm, which were used for qualitative analyses.

3.3 | Geochemical Isotopic Analyses

A total of 10 samples (Table S3) from evaporites (8) and mollusc shells (2) have been characterised for Sr. isotope signature at the Isotope Geochemistry Laboratory of the Department of Chemical and Geological Sciences at the University of Modena and Reggio Emilia. Analysis of $^{87}Sr/^{86}Sr$ was conducted using a multicollector inductively coupled plasma mass spectrometer

(HR-MC-ICPMS Thermo Scientific Neptune) at the Centro Interdipartimentale Grandi Strumenti of the University of Modena and Reggio Emilia. The methodology for sample processing followed the procedure outlined in Reghizzi et al. (2018) and Argentino et al. (2021). Strontium isolation from sample solutions was achieved using Eichrom Sr-SPEC resin SR-B50-A. Sample solutions were introduced into the Neptune via a PFA 100 μL/min nebulizer and a quartz cyclonic + Scott type spray chamber. The NIST SRM 987 served as the external standard. Normalisation of all values was done with respect to the NIST SRM 987 value of 0.710248, as used by McArthur (1994) and McArthur et al. (2001) as the reference standard for constructing the global marine seawater Sr. curve. Analytical errors are provided as both 2se (2-standard error or within-run error) and 2-sigma (i.e., 2se propagated with the NIST SRM 987 reproducibility).

3.4 | Subsurface Data

The stratigraphic correlation between the Albanides foredeep and the Apennine foreland was achieved through a review of four VIDEPI seismic profiles (B-443, M13, D444, F76-04) and three boreholes (Sparviero 001, Sparviero 001 bis and Gargano Mare 001), three VIDEPI boreholes previously interpreted by Manzi et al. (2020) (Eterno 001, Famoso 001 and Stella 001), the ADS-02 profile (Argnani 2013), and the geological section "4" (Shërbimi Gjeologjik Shqiptar 2002). Interpretation of well logs and onshore peri-Adriatic data allowed calibration of seismic profiles by identifying key seismic reflectors, such as the Messinian erosional surface (MES) and/or the evaporites. In addition, other VIDEPI boreholes previously investigated by Manzi et al. (2020) were also reported and considered for interpretation. Due to the presence of an erosional hiatus of variable amplitude, no MSC-related deposits are found in a small group of boreholes including: Cigno Mare 001, Gondola 001 bis, Grazia 001, Giuliana 001, Jolly 001, Rovesti 001, Imago 001, Picchio 001, Medusa 001, Rosaria Mare 001, Giove 001, Giove 002 and Merlo 001.

4 | Results

4.1 | The Rubjekë Section (R; 41°24′2.10″N; 19°35′55.42″E)

4.1.1 | Physical Stratigraphy

The Rubjekë section (Figure 2A), around 90 m-thick, is located few tens of meters north of the homonymous village and records the uppermost Miocene succession of the Preze monocline (Figure 1). Two informal units can be distinguished along the entire succession, as follows:

Pre-evaporitic units – it includes a lower interval made of weakly cemented silty-sandstones interbedded with up to 8 biocalcarenitic horizons (Figure 2B,C), each 20–30 cm thick belonging to the uppermost Rada Formation (Prillo and Hasanaj 2002). The horizons contain marine fossil assemblages with bivalves, gastropods, coralline algae, miliolids and bryozoans, whereas the interbedded silty sandstones show well-preserved oyster valves, particularly abundant above the first biocalcarenitic layer. These features point to an open marine environment, in agreement with the description of the top Rada Formation by Prillo and Hasanaj (2002). The Rada Formation passes upward to an interval, about 45 m thick, consisting of poorly cemented blue-grey marls barren of macrofossils referable to the Mengaj Formation (Prillo and Hasanaj 2002), in turn capped by the Gyps-Sharrë Gypsum unit.

Gyps-Sharrë Gypsum unit (GSG) – it consists of giant primary bottom-grown twinned selenite crystals, reaching up to 2 m across (Figure 2D–F), similar to those found in the lowermost two beds of the Primary Lower Gypsum unit (Lugli et al. 2010) in the Vena del Gesso basin (Northern Apennines). The thickness of the unit is 4 m and although the base is not well exposed, the vertical orientation of the gypsum crystals reconstructed from lateral (Figure 2D,F) and top (Figure 2E) views matches the regional dip of the Preze monocline. Thus, a conformable contact with the underlying terrigenous unit is expected. Conversely, the top of the evaporites is truncated by an erosional surface that developed at the end of the PLG deposition, albeit a more recent reshape cannot be excluded. According to the geological map (Shërbimi Gjeologjik Shqiptar 2002), these evaporites are overlain by fine-grained Pliocene deposits (not outcropping).

4.1.2 | Biostratigraphy

Micropaleontological analyses carried out in blue-grey marls contain a scarce and poorly preserved microfossil record that does not allow biostratigraphic determination.

4.1.3 | $^{87}Sr/^{86}Sr$ Isotope Stratigraphy

The geochemical analyses on the giant selenite crystals yielded an $^{87}Sr/^{86}Sr$ value of 0.708952 ± 0.000014 (Table S3) compatible with stage 1 of the MSC.

4.2 | The Guri i Cifutit Section (G; 40°30′38.19″N; 19°27′43.43″E)

4.2.1 | Physical Stratigraphy

The Guri i Cifutit section (Figure 3A,B), measured in an abandoned quarry located few kilometres north of Vlora, is ~60 m-thick and shows the most complete evaporitic Messinian succession within the Peri-Adriatic depression (Figure 1C). Two units can be distinguished.

Gyps-Sharrë Gypsum unit (GSG) – This unit is more than 40 m-thick and consists entirely of primary gypsum characterised by an alternation of massive selenite (Figure 3C), banded selenite (Figure 3D,E) and branching selenite facies (Figure 3F) with thin shale horizons forming 3–4 depositional cycles. A very distinctive feature of this unit, which is barren of fossils, is the presence of dm-thick bands truncated at the top by dissolution surfaces (Figure 3C) in the massive selenite. These evaporites lay above the pre-evaporitic Mengaj/Rada Fm, although the contact is not visible in the quarry, and are truncated on top by an

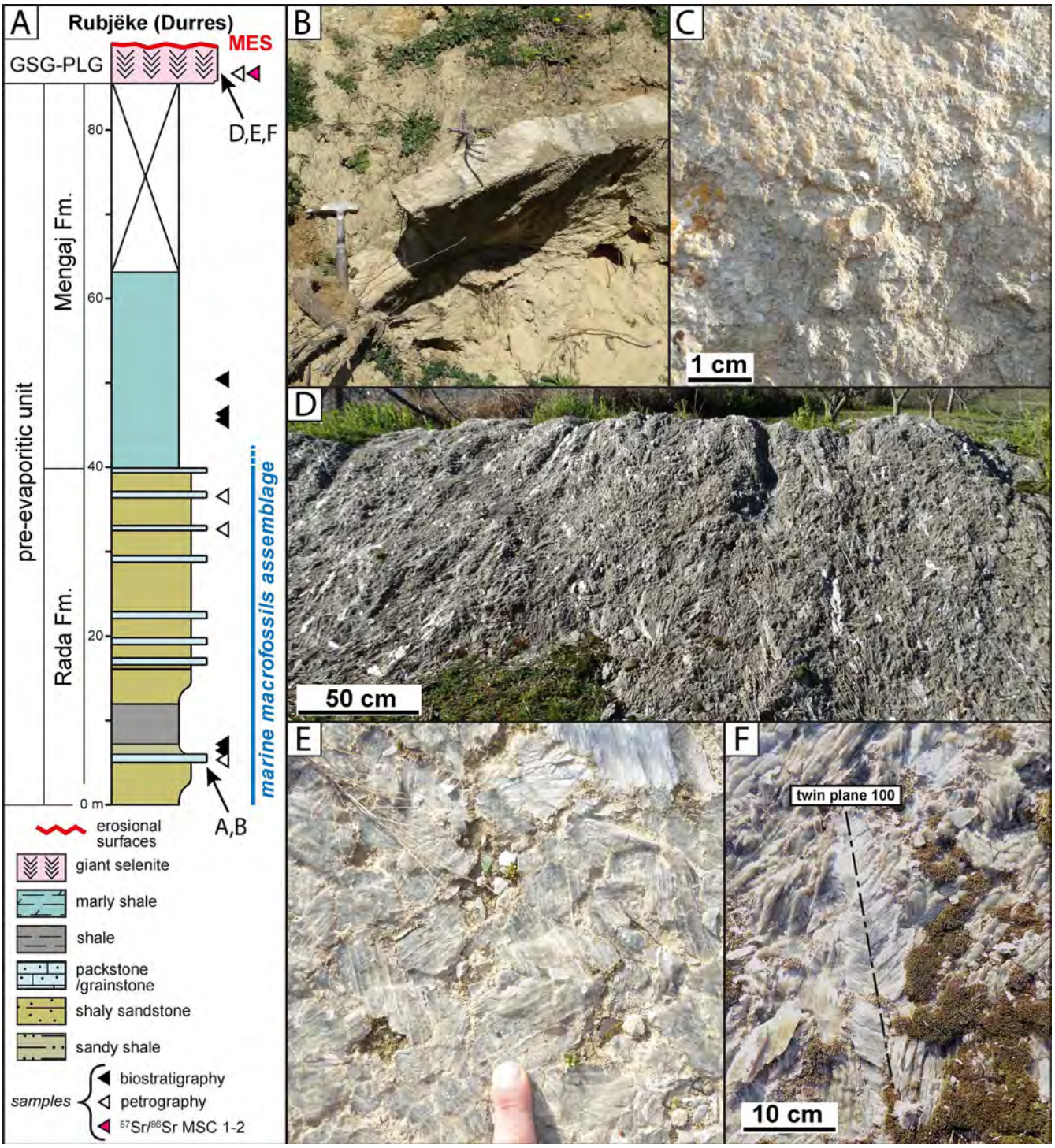


FIGURE 2 | Rubjëke section: (A) Lithostratigraphic log and paleontological findings and sample location. (B) Lowermost biocalcarenite bed. (C) Close-up of the fossiliferous content of the biocalcarenitic bed in B. (D) Truncation surface at the top of the Evaporitic Unit (GSG, Gyps Sharre Gypsum). Top (E) and lateral (F) detailed views of the giant twinned gypsum crystals of the GSG unit.

angular discordance; the GSG unit dips SE, whereas the overlying unit dips NE.

Blue marl unit (BMU) – this unit consists of a lower finer-grained portion, with up to 10 m-thick, of bluish shaly-marls containing shallow-water marine fauna represented by solitary hexacorals in the marly limestone (*Scleractinia*; Figure 3G) and *Cardium* and *Muricopsis* shells in the shale intervals (Figure 3H). The base (not well exposed) is marked by a strongly altered marly limestone layer with abundant plant frustules. The top portion consists of a coarser-grained layer with several sandstone beds, up to 1 m-thick, interbedded with bluish marls.

4.2.2 | Biostratigraphic Analyses

Micropaleontological analyses carried out in the shales of the BMU reveal the presence of *Sphaeroidinellopsis seminulina*

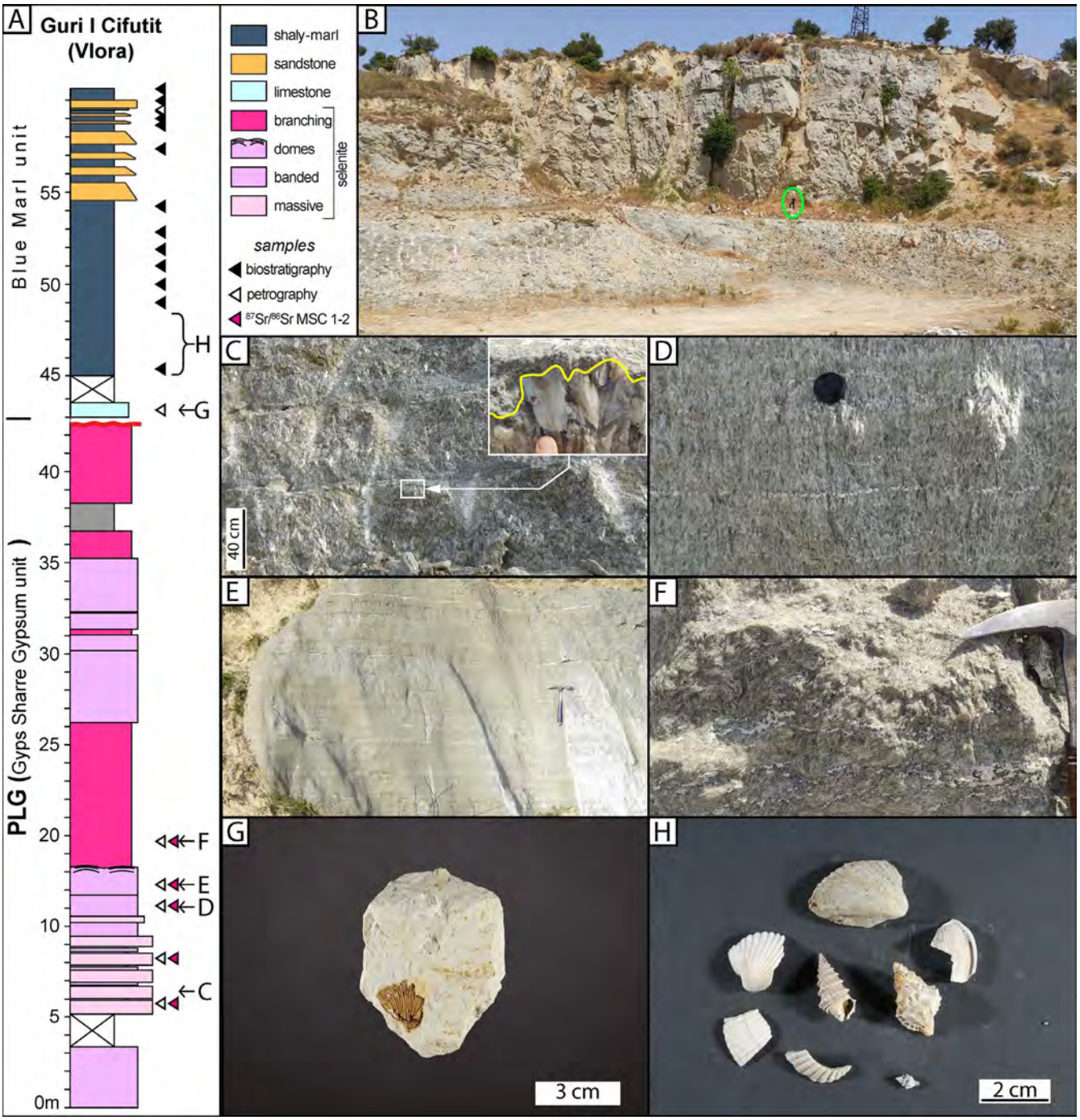


FIGURE 3 | Guri i Cifutit (Vlore) section. (A) Lithostratigraphic section with sample loaction. (B) Panoramic view of the Guri I Cifutit quarry (encircled person for scale). (C) The banded-massive selenite facies with close-up of centimetric crystals truncated by a dissolution surface. (D) Coarse banded selenite (camera lens cap for scale). (E) Banded selenite. (F) Branching selenite. (G) Hexacoral within marly limestone. Marine malacofaunas with bivalves (H) Marine malacofaunas with bivalves and gastropods recognized in the Pliocene Blue clays.

that, together with the absence of *Globorotalia margaritae* and *Globorotalia puncticulata*, could suggest an early Pliocene age.

4.2.3 | Geochemical Isotope Analyses

A total of 5 samples, including the different primary selenite facies, provided $^{87}Sr/^{86}Sr$ values ranging from 0.708928 ± 0.000006 to 0.708950 ± 0.000006 (Table S3) with an average value of 0.708939. These values fall in the field of the early stage of the MSC.

4.3 | The Currilla Section (C; 41°19′25.36″N; 19°25′33.26″E)

4.3.1 | Physical Stratigraphy

The Currilla section, around 450 m-thick, crops out along the coast of Durres along the eastern flank of the Durres-Palla anticline, whose axial plane is located just off the coast (Figure 1C). Based on lithofacies and biofacies, from base to top, up to 4 units can be distinguished (Figure 4A,B).

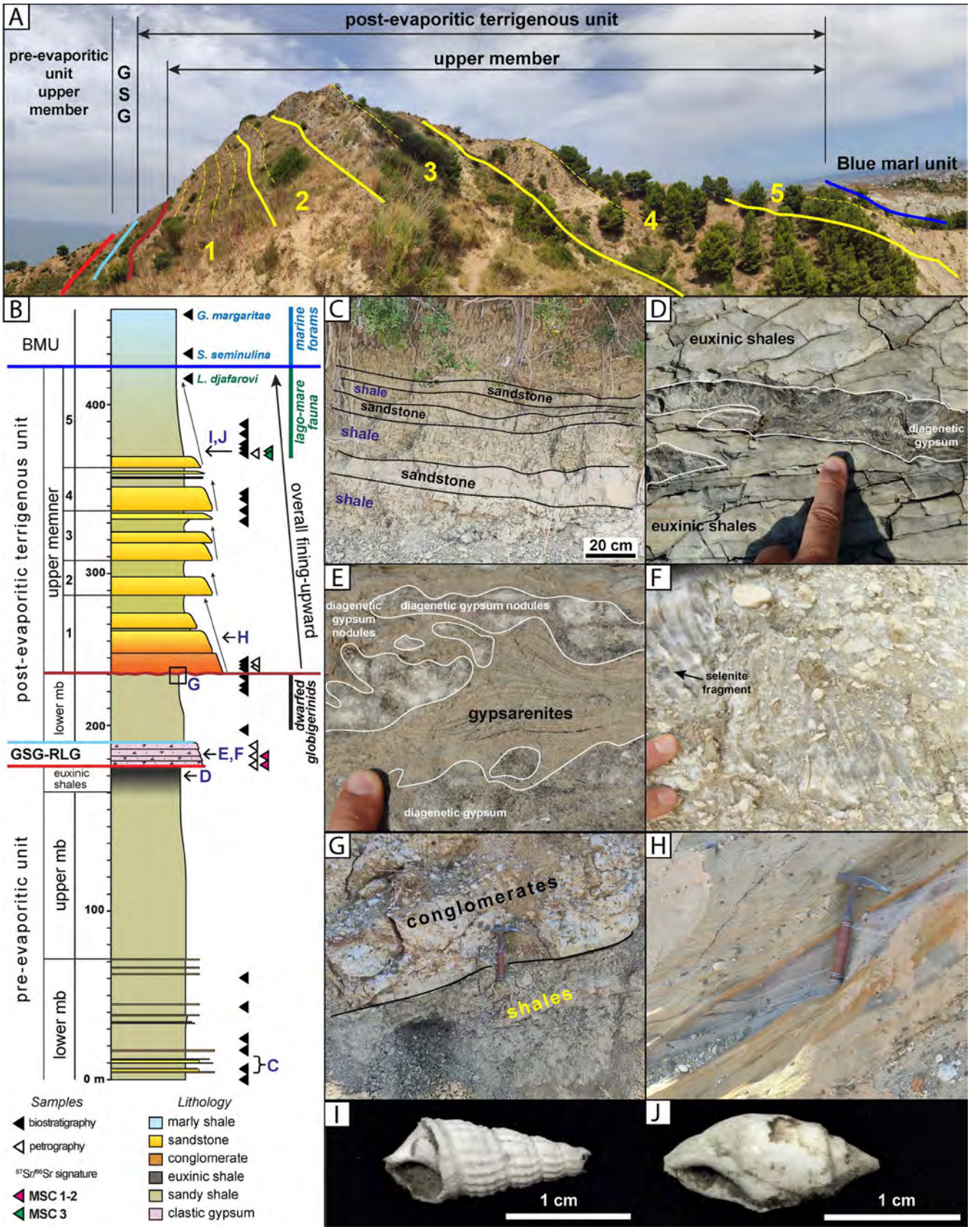


FIGURE 4 | Currilla section (Durres). (A) Panoramic view of the Currilla section showing the main 5 sedimentary cycles given by the alternation of coarse-grained and fine-grained horizons. (B) Lithostratigraphic log with main paleontological findings and sample location. (C) Thin-bedded turbidites at the base of the Lower Terrigenous Unit (LTU). (D) Euxinic shales with diagenetic gypsum crystals. (E) Gypsarenite with diagenetic gypsum nodules. (F) Gypsarenite with primary gypsum clasta (G) Abrupt passage between the Intermediate terrigenous unit (ITU) and the basal conglomerate of the Upper Terrigenous Unit (UTU). (H) Cross-bedded sandstones of the UTU. (I) Melanopsis narzolina. (J) Melanoides curvicosta.

Pre-evaporitic unit – This unit is more than 180 m-thick and is characterised by an overall fining-upward trend; its lower portion consists of an alternation of sandstone and shale (Figure 4C) with rare, thin (< 0.5 m) microconglomeratic and conglomeratic layers; these deposits pass gradually upward to an interval characterised by shale with minor sand beds; at the top, a poorly-exposed interval (~5 m-thick) of dark euxinic shale with secondary diagenetic nodules of macrocrystalline gypsum is present (Figure 4D). Other diagenetic nodules are found in the gypsarenite deposits (Figure 4E). These nodules probably formed by the rehydration of anhydrite during exhumation. Differently from what was observed in the previous sections, the unit is characterised by higher terrigenous content and is devoid of macro and microfossils.

Gyps-Sharrë Gypsum unit (GSG) – the evaporitic unit consists of ~12 m-thick alternation of laminated gypsarenite/gypsrudite and shale. Differently from the previous sections, no primary gypsum facies are present, only clastic. The original lamination is locally deformed by whitish diagenetic microcrystalline gypsum nodules (Figures 4E and 5A,D). Both macro- and microcrystalline diagenetic nodules show no evidence of anhydrite precursor (Figure 5B,E). Carbonate clasts, as a minor component of the gypsrudite, show cubic moulds filled by secondary gypsum (Figure 5C,F).

Post-evaporitic unit – This unit overlying the clastic evaporites is not present in the previous sections and can be separated into two sub-units. The lower sub-unit, about 40 m-thick, is made of sandy shale resting conformably overlying the evaporitic unit. At its top the unit is truncated by the erosional base of the upper sub-unit (Figure 4F). The upper sub-unit is 180 m-thick and is characterised by a rhythmic alternation of coarse- and fine-grained deposits forming 5 main sharp-based, fining-upward sedimentary cycles (Figure 4A,B) organised in an overall fining- and thinning-upward stacking pattern (Figure 4B). In the basal cycle the coarse-grained interval is a 10 m-thick conglomerate-sandstone body including in its lower part dm-sized pebbles that can be laterally traced in outcrop for more than 4 km along the coast north of Durres. In the overlying cycles the basal portion consists of cross-bedded sandstone (Figure 4G,H). Fossils (gastropod and bivalve shell fragments) are present only in the upper portion of the shale horizons (Figure 4I,J).

Blue marl unit (BMU) – the light brown fossiliferous shaley-marl at the top of the post-evaporitic unit passes upward to a 20 m-thick fine-grained unit made up of bluish marly shale.

4.3.2 | Biostratigraphic Analyses

The lower portion of the pre-evaporitic unit does not contain fossils. In the post-evaporitic unit, two fossiliferous intervals with distinct characteristics have been identified. The lower one is characterised by very rare dwarfed globigerinids, unidentifiable because of their extremely small size, the poor state of preservation and the abundant recrystallization. The upper one, occurring immediately above the last sandstone bed (samples H, I), is characterised by a faunal assemblage with hypohaline gastropods including *Melanopsis narzolina* (d'Archiac in Viquesnel, 1846; Figure 4I) and *Melanoides curvicosta* (Deshayes, 1835; Figure 4J). This fossil assemblage is commonly identified in the Lago-mare deposits of stage 3 (Orszag-Sperber 2006). In the uppermost portion, just before the transition with the bluish-grey marly shale (Figure 4A), some small globigerinids associated with valves of *Loxocorniculina djafarovi* have been recognised; the latter species is a typical Lago-mare marker (Gliozzi 1999; Bassetti et al. 2003; Roveri et al. 2008a; Roveri, Flecker, et al. 2014). In contrast, the sample immediately above, in the Blue Marls unit, shows an organic fraction composed of planktonic foraminifera and a few benthic tests (P/B >> 1). The planktonic assemblage consists of *Orbulina universa* (d'Orbigny, 1839), *Globigerina bulloides* (d'Orbigny, 1826), *Globigerina falconensis* (Blow, 1959), *Sphaeroidinellopsis seminulina* (Schwager, 1866), *Neogloboquadrina acostaensis* (Blow, 1959) and some rare *Globorotalia scitula*, pointing to open marine conditions. Finally, the uppermost sample shows a similar planktonic assemblage, except for the rare presence of *Globorotalia margaritae* (Bolli and Bermudez, 1965). Accordingly, the post-evaporitic unit can be ascribed to the uppermost Messinian and the Blu Marl unit to the lower Zanclean.

4.3.3 | Geochemical Isotopic Analyses

Two different populations of $^{87}Sr/^{86}Sr$ values can be distinguished for this section (Table S3). The 2 samples collected in the clastic gypsum of the EU show values of 0.708928 ± 0.000014 and 0.708952 ± 0.000014, typical signature of the Lower Evaporites (stage 1 and 2). Conversely, the 2 samples of the hypohaline fauna found in the UTU provided more depleted values (0.708777 and 0.708786 ± 0.000006) compatible with the uppermost Messinian Lago-mare. See Table S2 for details.

5 | Discussion

5.1 | Correlation of PAD Sections

The Gyps-Sharrë Gypsum Fm. cropping out in the Rubjekë and Guri i Cifutit sections consists of bottom-grown primary evaporites that, on the basis of their depositional facies, similar to those described by Lugli et al. (2010), and of their $^{87}Sr/^{86}Sr$ isotopic signature, can be ascribed to the Primary Lower Gypsum unit. Both sections show an incomplete succession, truncated at the top by an unconformity that can be correlated with the Messinian erosional surface (MES; Figure 6). The presence of the giant selenite facies, a stratigraphic marker at the Mediterranean scale of the first two precessional cycles (Lugli et al. 2010) in the lowermost gypsum cycles, suggests that the base of the PLG in the Rubjekë section is conformable. Moreover, the gypsum selenite overlies a shale and biocalcarenite succession deposited in a shallow-water shelfal environment; thus, in good agreement with the maximum depth of 200 m estimated for the overlying PLG unit (Lugli et al. 2010).

In the Guri i Cifutit section the local base of the evaporitic unit does not crop out and it is not possible to know if the basal cycles are present, as documented for the Kavaje section (Bigi et al. 2024). However, the scarce deformation, good preservation

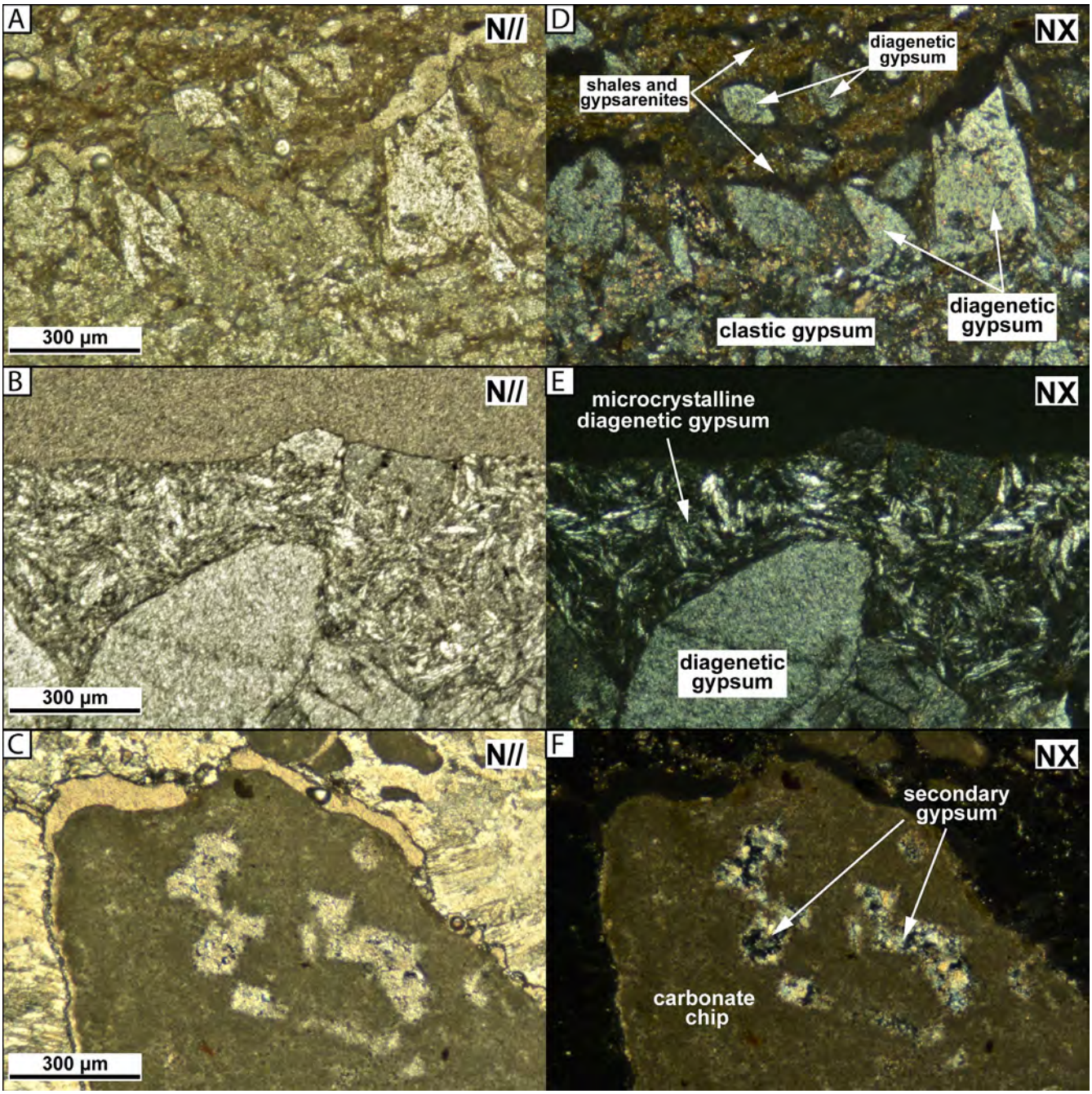


FIGURE 5 | Thin sections of clastic evaporites from the Currilla (C; Durrës) section. Diagenetic gypsum within a gypsarenite layer viewed at parallel (A) and crossed nicols (D). (B) Contact between large crystal of diagenetic gypsum and lenticular microcrystalline gypsum viewed at parallel (B) and crossed nicols (E). (C) Cubic and hexagonal moulds within a carbonate clast filled by secondary gypsum viewed at parallel (C) and crossed nicols (F).

and lateral continuity of the evaporites suggest a conformable boundary above the pre-evaporitic deposits. The peculiar evaporitic facies known as branching selenite, which is a pivotal stratigraphic marker appearing only from the 6th precessional cycle upward in the PLG unit (Lugli et al. 2010), has been recognised in the Guri i Cifutit section. The overlying post-evaporitic succession, containing *Sphaeroidinellopsis seminulina*, corals and marine malacofaunas can be interpreted as a shallow-water, open marine lower Pliocene unit.

Conversely, the Gyps-Sharrë Gypsum Fm. outcropping in the Currilla section shows significant differences; in fact, it is characterised by: (i) a slight erosional base above a dark shale barren unit (not found in the other sections); (ii) the complete lack of primary evaporitic deposits; (iii) the only occurrence of clastic evaporite facies; (iv) the presence of a conformably overlying terrigenous unit (not found in the other sections), including in its upper portion hypohaline faunal assemblages ascribable to the Lago-mare; (v) the presence above the terrigenous unit of a bluish marl unit with marine fossils, of possibly Zanclean age. The erosional base, the exclusive occurrence of clastic facies, and the isotopic values (typical of stages 1–2) allow us to confidently correlate the evaporites of the Currilla section to the Resedimented Lower Gypsum unit (RLG), that is commonly

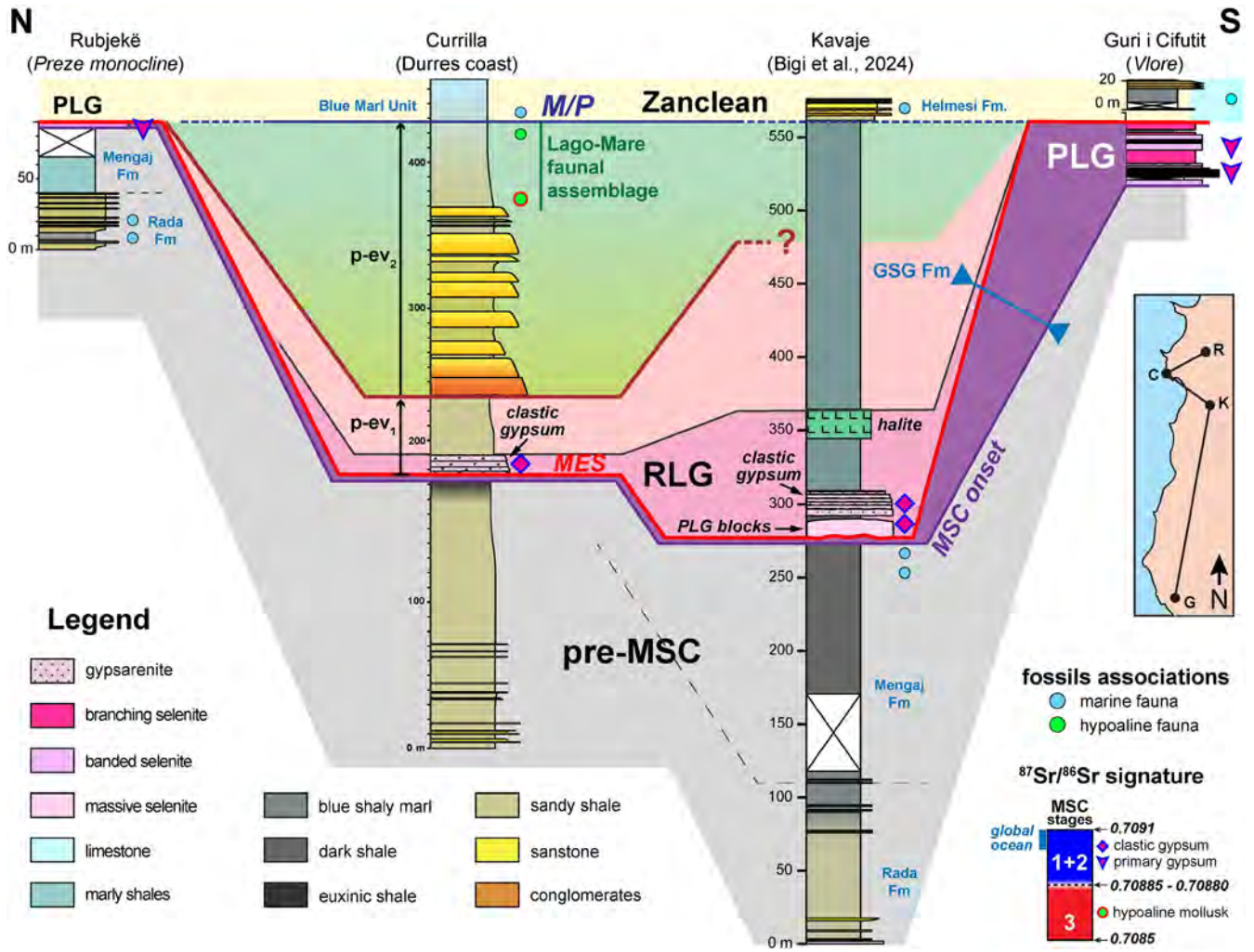


FIGURE 6 | Correlation lithostratigraphic sections of the Peri-Adriatic Depression (PAD) showing the distribution of paleontological findings and the Strontium isotope results.

observed in deep basinal successions of stage 2 (Figure 6). The presence of turbiditic siliciclastic deposits and the absence of macrofossil-rich calcarenites in the underlying pre-evaporitic succession suggest a deeper environment with respect to the previous sections also before the crisis. Although a detailed bio and magneto-stratigraphic study is lacking, the presence of euxinic shales totally devoid of foraminifera below the clastic evaporites can be tentatively interpreted as corresponding to the Foraminifer Barren Interval (FBI; Manzi et al. 2018, 2021), i.e., the deep-sea time-equivalent of the Primary Lower Gypsum (stage 1), that is missing in the Currilla section. Thus, the erosional base of the clastic evaporites can be traced in shallow settings above the PLG unit and correlated with the Messinian erosional surface. Another exclusive aspect of the Currilla section is the presence above the evaporites and below the Pliocene marine Blue Marl Unit of a thick terrigenous succession including typical Lago-mare ostracod (*L. djafarovi*) and mollusc (*Melanoides* and *Melanopsis* spp.) assemblages with stage 3 isotopic signatures and showing a gradual transition to the early Zanclean, as indicated by the presence of *S. seminulina* (MPl1 zone; Lirer et al. 2019).

Summarising, we can identify two sectors of the peri-Adriatic depression, namely the inner part of the Durres area (Rubjekë section) and the Vlora area (Guri i Cifutit section), which before and during the MSC were characterised by relatively shallow-water environments, hosting PLG unit deposition during stage 1 (Figure 7). In contrast, the outermost sector of the PAD, now cropping out in the Durres coast (Currilla section), must have been much deeper before and during the crisis, hosting the accumulation of only clastic evaporitic deposits during stage 2 (Figure 6). The Kavaje section, the only record in Albania of the MSC onset within euxinic shales (Bigi et al. 2024), can thus be interpreted as an intermediate depositional setting (Figure 6). In fact, in situ PLG evaporites are absent in the Kavaje area, but the RLG unit appears very different from the Currilla section, showing more coarse-grained facies (gypsrudites), chaotic deposits (comprising mountain-size PLG olistoliths), and primary halite (Bigi et al. 2024), pointing to a shorter distance from the source areas.

The re-interpretation of the geological Section 4 of the Albanian geological service (Shërbimi Gjeologjik Shqiptar 2002) after the above-described considerations clearly summarises the correlation between the inner and outer depozones of the peri-Adriatic depression (Figure 7). The uplift of the Preze monocline in the inner part of the PAD generated shallow-water environments that favoured the evaporitic

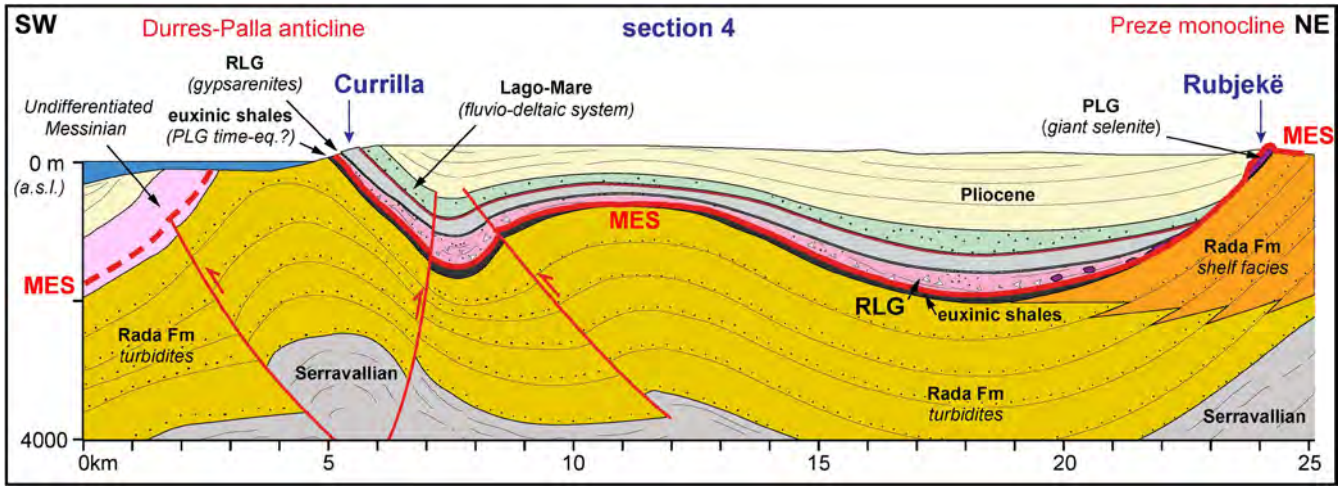


FIGURE 7 | Re-interpretation of the Geological Section 4 of the Shërbimi Gjeologjik Shqiptar (2002; see location in Figure 1A). The section crosses the investigated successions at the structural highs of the Preze monocline and the Durres-Palla anticline, showing the arrangement of the deposits of the 3 stages of the crisis.

precipitation during stage 1 (Rubjekë wedge-top, PLG unit). During the uplift, the area of the current Durres-Palla anticline was still characterised by a foredeep context, allowing the accumulation of clastic evaporites (RLG) in the subsequent stage 2. These clastic evaporites result from erosion or total dismantling of the primary evaporites accumulated during stage 1. This is because the continuous growth of structures, such as the Preze monocline, has caused slope instability and the possible subaerial exposure of the PLG unit, generating the Messinian erosional surface. The Currilla section also testifies that, compared to the other sections, a relatively deep-water setting persisted even during stage 3, with the deposition of a thick Lago-mare terrigenous succession, and the basal Pliocene, in which the almost exclusive presence of planktonic foraminifers indicates a pelagic sedimentation.

5.2 | The Correlation of the Currilla Section With the Mediterranean Sections

The terrigenous post-evaporitic succession overlying the RLG unit in Currilla section exhibits lithofacies, biofacies, and stacking patterns that allow a correlation with stage 3 of the Central and Western Mediterranean (Dabrio and Polo 1995; Roep et al. 1998; Roveri et al. 1998; Krijgsman et al. 2001; Fortuin and Krijgsman 2003; Bassetti et al. 2004; Roveri et al. 2008b, 2009; Omodeo-Sale' et al. 2012; Andreetto et al. 2021; Roveri et al. 2026). Like the Northern Apennines and the Southern Spain successions (Figure 8), the stratigraphic pattern of the post-evaporitic unit of the Currilla section records the cyclic activation/deactivation of fluvio-deltaic systems, indicated by the deposition of large volumes of coarse-grained silicoclastic sediments. These elements allow the attribution of the upper member to stage 3.2 (Figure 8; p-ev$_2$ unit sensu (Roveri et al. 1998)), whose base, dated at 5.42 Ma, records a strong variation of the precipitation regime in the peri-Mediterranean area (Roveri et al. 2008b; Roveri et al. 2026). This interpretation is confirmed by the presence of Lago-mare faunal assemblages and in particular by the occurrence of *L. dijafarovi* (a stratigraphic marker of stage 3.2) at the top of the succession, which, together with their depleted $^{87}Sr/^{86}Sr$ value, indicates a period of greater isolation of the Mediterranean from the Atlantic Ocean and a simultaneous intensification of exchanges with the Paratethys (Orszag-Sperber 2006; Rouchy and Caruso 2006; Roveri et al. 2008b; Roveri et al. 2026).

5.3 | Onshore—Offshore Correlation

Through the correlation of the Albanian onshore data with the seismic data from the Adriatic offshore (B-443, M-13, D-444, F76-04, ADS-02; Figures 1A and 9A), a composite geologic section has been reconstructed (Figure 9B), which highlights the distribution of MSC deposits (mainly evaporites) from the Peri-Adriatic depression to the Adriatic foreland (Figure 9A). Profile ADS-02 identifies a seismic unit of Messinian age (Argnani 2013), which is involved to the east in the Durres-Palla anticline (Section 4; Figures 7 and 9B). Profile ADS-02 connects westward with seismic section F76-04, which reveals the northwestern boundary of the Southern Adriatic basin and can be calibrated with the Sparviero 001-001bis (Figure 9C) and Gargano Mare 001 (Figure 9D) boreholes. In this section the continuation of the Messinian unit identified by Argnani (2013) to the Sparviero 001 anticline can be recognised. Here, the Sparviero 001 and 001bis boreholes cross the Messinian succession between 1700 and 1860 m depth (Figure 9C). Between 1700 and 1760 m, the resistivity log is characterised by a "spiky" pattern (Figure 9C) suggesting the alternation of thin (m-thick?) gypsum beds (high resistivity) with arenitic and shale deposits (low resistivity). This "spiky" pattern, that can be referred to the RLG unit, clearly differs from the "blocky" one that allowed to recognise the PLG unit (Manzi et al. 2020), and that can be observed in the Eterno 001, Famoso 001 and Stella 001 boreholes (Figure 9E).

Moving westward along transect F76-04, the Gargano Mare 001 borehole intercepts the offshore extension of the Gargano structural high (Figure 9B), where an erosional hiatus is present between the Tortonian shelf marls and the Pleistocene carbonate deposits (Figure 9D). The same erosional surface can be

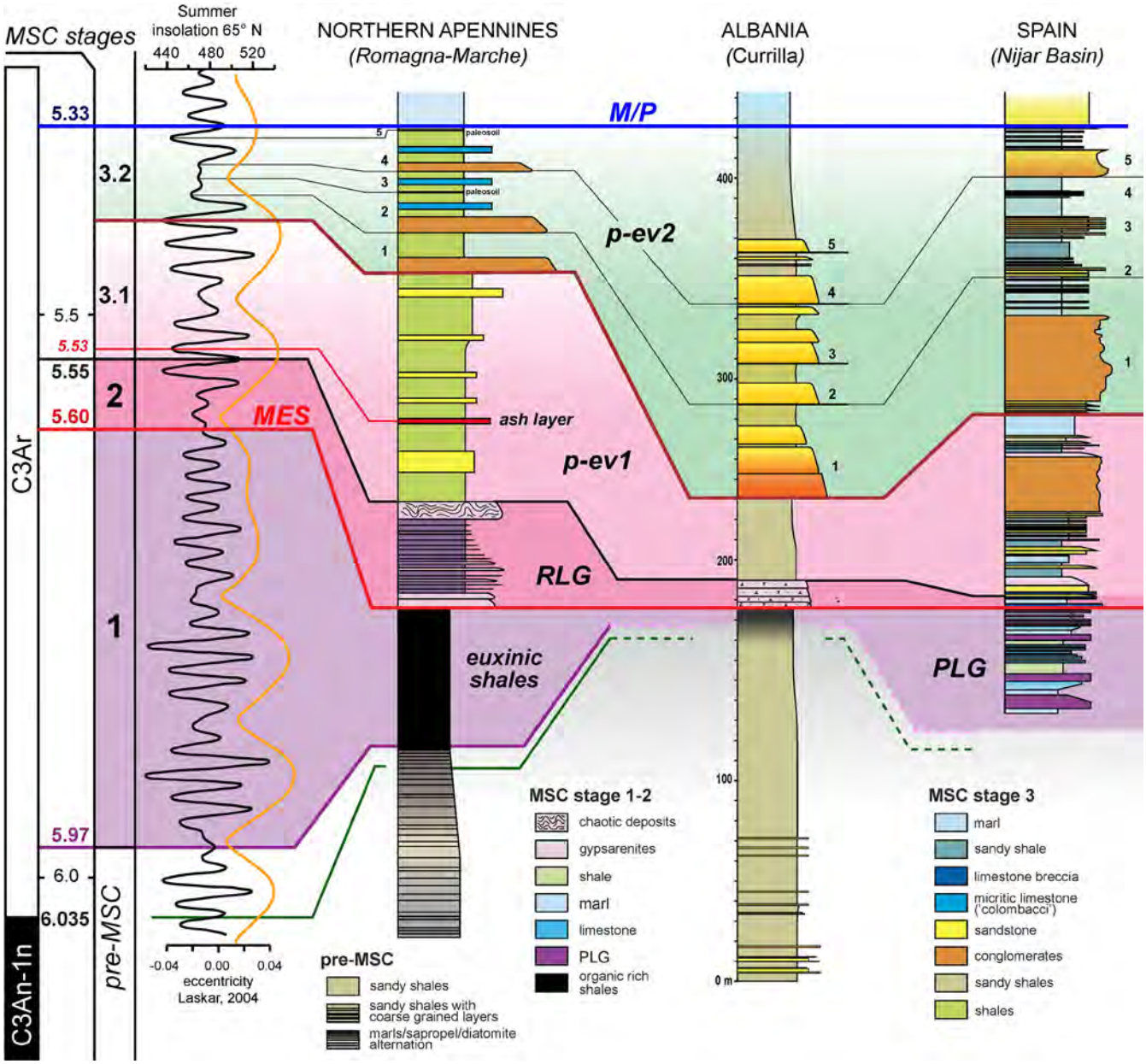


FIGURE 8 | Astronomical tuning of the Currilla section and stratigraphic correlation with the Northern Apennines composite section (modified from Roveri, Flecker, et al. 2014) and Barranco de Los Castellones section (Nijar Basi, Southern Spain; from Omodeo-Sale' et al. 2012).

followed in the seismic sections D-444 and M-13, but since no boreholes are available, the extension of the hiatus cannot be determined. Section B-443 was calibrated by boreholes Stella 001, Famoso 001, and Eterno 001, previously interpreted by Manzi et al. (2020; Figure 9E). Here, the PLG unit, developed above a shelfal carbonate (Bolognano Formation) and foreland ramp mud (Schlier Formation) succession, is truncated on top by the Messinian erosional surface (MES). The reflector corresponding to the MES can be correlated with the unconformity present in transects D-44 and F17-M13 (Figure 9B).

The calibration of the seismic section F76-04 through the Sparviero 01 borehole allows us to interpret the Messinian seismic unit identified by Argnani (2013) and, consequently, to reconstruct a general framework extended from the Apennines to the Albanides according to the following points:

- The Southern Adriatic basin is characterised by a strong seismic reflector that can be followed along the sections F76-04 and ADS-02 representing the clastic evaporites unit (RLG) drilled in the Sparviero 01 borehole; eastward this reflector can be traced up to the Durres coast, where the clastic evaporites outcrop in the Currilla section.
- In agreement with Manzi et al. (2020), no evaporite deposits are found above the Gargano structural high. Here an unconformity surface that can be interpreted as the MES truncates the Tortonian (Gargano-Mare 001; Figure 10C), or even the Mesozoic units, and is sealed by the Plio-Quaternary deposits.
- The PLG deposits, drilled by the Stella 001, Famoso 001, and Eterno 001 boreholes, appear only north-west of the

Gargano high (Figure 10B). they overlie a succession including carbonate (Bolognano Fm) to hemipelagic marl deposits (Schlier Fm). These evaporites are comparable with those of the Rubjekë and Guri i Cifutit sections resting on the shelfal deposits of the Rada Formation.

– The fine-grained deposits above the RLG unit in the Sparviero 001 borehole could tentatively be ascribed to the Lago-mare stage (Figure 10D); although the lack of paleontological data does not allow us to confirm this interpretation.

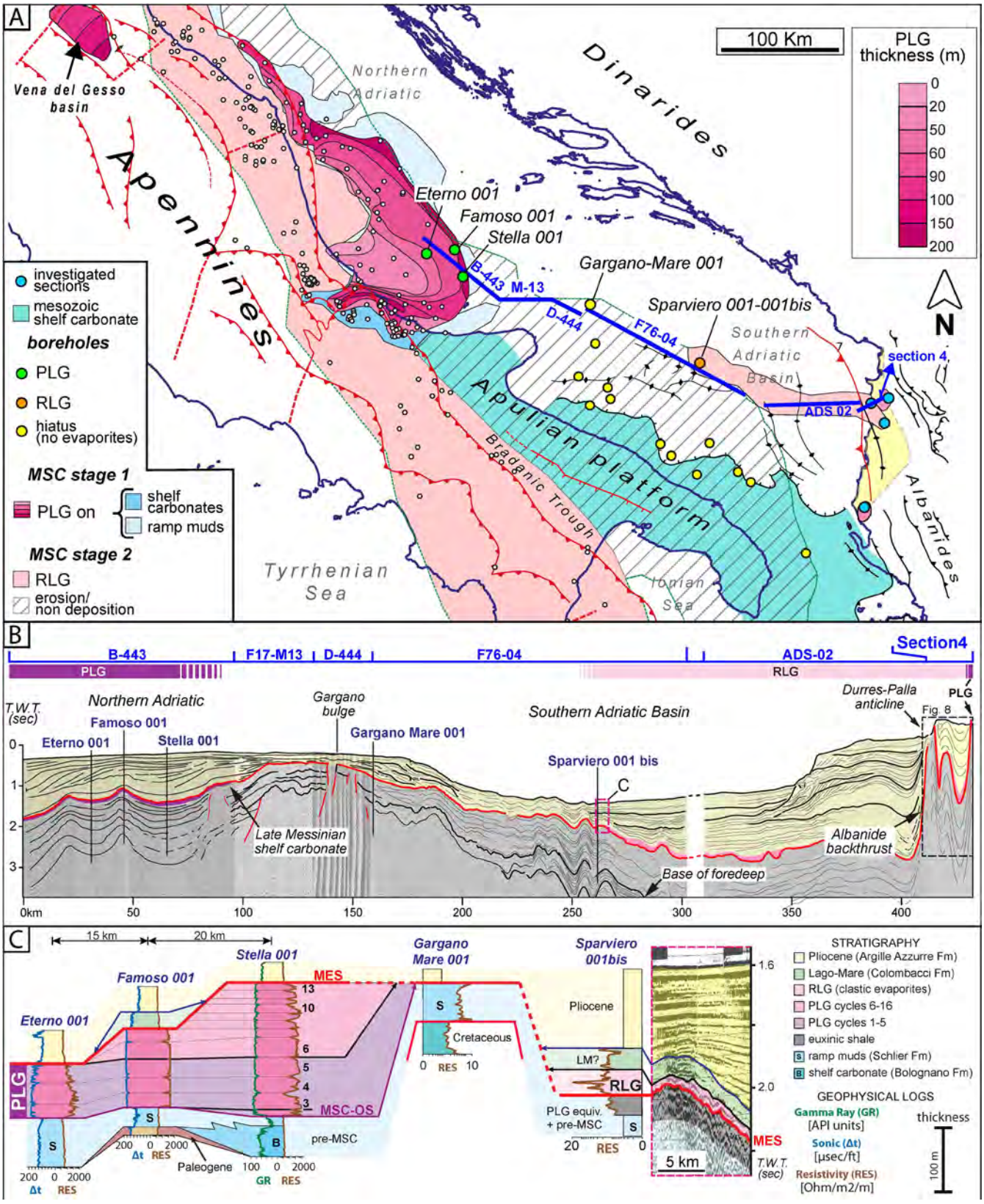


FIGURE 9 | Legend on next page.

FIGURE 9 | (A) Distribution of evaporites in the Adriatic Basin (modified from Manzi et al. 2020) and location of seismic lines, exploratory boreholes, and stratigraphic sections. The PLG unit is present both in wedge-top contexts of the Apennine (Vena del Gesso) and Albanian (inner sector of the PAD) chains and in the Adriatic foreland region. The RLG deposits, on the other hand, are located in the Apennine foreland and south-Adriatic basin (Albanian foredeep). The Gargano structural high and the Apulian Platform represent areas of erosion/non-deposition. (B) Composite seismic section (location in Figures 1A and 9) correlating the Adriatic foreland with the Albanian onshore (peri-Adriatic depression). Light blue indicates the pre-MSC sediments, whereas the Plio-Quaternary deposits are shown in yellow. The depocenters of the PLG and RLG units are highlighted along the section. (C) The PLG depocenter in the Adriatic foreland intercepted by the Eterno-001, Famoso-001 and Stella-001 boreholes (modified from Manzi et al. 2020). Geophisical logs allow to distinguish primary vs clastic evaporitic deposits. A Magnification on the seismic section intercepted by the Sparviero 001 bis borehole is also provided.

From these considerations it follows that the distribution of the Messinian evaporites in the Adriatic basin largely reflects the Mesozoic palaeogeography. In particular, the Southern Adriatic basin (i.e., the Albanides foredeep basin since the Alpine orogeny; Argnani 2013), represents an area already depressed at the end of the Cretaceous, where deep sea sediments accumulated continuously since the Oligocene onwards (Argnani et al. 1996; Argnani 2013). During stage 1 the precipitation of the PLG unit occurs only in shallow-water settings, which are located along the section: (i) in the wedge-top basins (Figures 8 and 10A), (ii) in the Albanides thrust-front (Rubieke and Guri i Cifutit Sections) and (iii) in the Adriatic foreland (Stella 001, Famoso 001, Eterno 001; Figure 10A,B). The excellent preservation of the PLG evaporites in the latter sector is due to the rapid subsidence following the increased lithostatic load generated by the eastward migration of the Apennines (Manzi et al. 2020). In agreement with Manzi et al. (2020), the paleo-Gargano high represents the south-eastern sill delimiting the largest PLG basin of the Adriatic foreland. Moving southwards, in the southern Adriatic basin the PLG unit is replaced by euxinic shales, probably due to a greater paleodepth characterised by anoxic conditions not allowing the deposition of primary selenite (Manzi et al. 2007; Lugli et al. 2010; de Lange and Krijgsman 2010; dela Pierre et al. 2011). This basin hosted the deposition of evaporites only during stage 2 when the clastic gypsum of the RLG unit was accumulated (Figure 10A). This unit has been deposited from the edge of the peri-Adriatic depression up to the Sparviero 001 anticlines. The terrigenous unit representing the Lagomare deposits of stage 3 crossed by the Famoso 001 borehole (Adriatic foreland) and outcropping in the Currilla section (Albanides foredeep) could likely share the areal distribution of the RLG unit within the Southern Adriatic Basin.

5.4 | Mediterranean-Scale Implications

The Albanian record of the Messinian salinity crisis confirms the existence of three main depositional stages, each characterised by specific hydrological and environmental conditions. These stages broadly correspond to those recognised in other Mediterranean settings, with only minor differences.

5.4.1 | Environmental Conditions for the Primary Sulfate Precipitation

The deposition of primary sulphates during stage 1 occurred in two areas located in structurally elevated settings (wedge-top basin, Rubijeke; foreland, Guri i Cifutit). Based on the characteristics of the underlying deposits of the Rada Fm., these settings were likely relatively shallow, as documented in other marginal Mediterranean basins, Apennines (Roveri et al. 2003; Lugli et al. 2010; dela Pierre et al. 2011; Manzi et al. 2020), Sicily (Roveri et al. 2008b; Lugli et al. 2010), and Spain (Roveri et al. 2020). A shallow water setting is also consistent with the identification of Ribosomal RNA gene fragments from fossilised cyanobacteria in the Vena del Gesso basin (Panieri et al. 2010).

Based on biomarkes analyses, Natalicchio et al. (2021) suggested deposition from a stratified water body, although such conditions appear unlikely in shallow settings. Another debated issue concerns the contribution of oceanic water during the deposition of the stage 1 primary evaporites. A significant dilution effect by meteoric water, first proposed by Longinelli (1979) and supported by Sr. isotope analyses (Flecker and Ellam 2006; Roveri, Lugli, et al. 2014 and reference therein), has been recently reconsidered (García-Veigas et al. 2018; Aloisi et al. 2024; Ryan and Raad 2025; Gázquez et al. 2026).

Reghizzi et al. (2018) described the precipitation of the primary sulfates as a highly dynamic process, characterised by high-frequency (annual) cyclicity. Low salinity conditions have also been inferred from fluid inclusions analyses (Attia et al. 2004; Natalicchio et al. 2014; Evans et al. 2015; Costanzo et al. 2019), but more recently, Bigi et al. (2022) demonstrated that the primary gypsum precipitated from a marine brine that was later modified during tectonic processes and exhumation.

These apparently contrasting interpretations may reflect the limited resolution of some investigations, which provided averaged or mediated signals. In this context, the Guri I Cifutit record confirms the occurrence of short-term climate variability accompanying the precipitation of the Primary Lower Gypsum deposits.

5.4.2 | The Acme of the Salinity Crisis

The Albanian record of the salinity crisis shows that the primary sulfates underwent intense erosion and re-sedimentation under subaqueous conditions, as reconstructed in many Mediterranean basins. Gravity-driven deposits are documented only in the deeper settings, both onshore (Peri-Adriatic Depression) and offshore (Southern Adriatic basin). These clastic deposits locally include small halite deposits (e.g., Kavaje; Bigi et al. 2024).

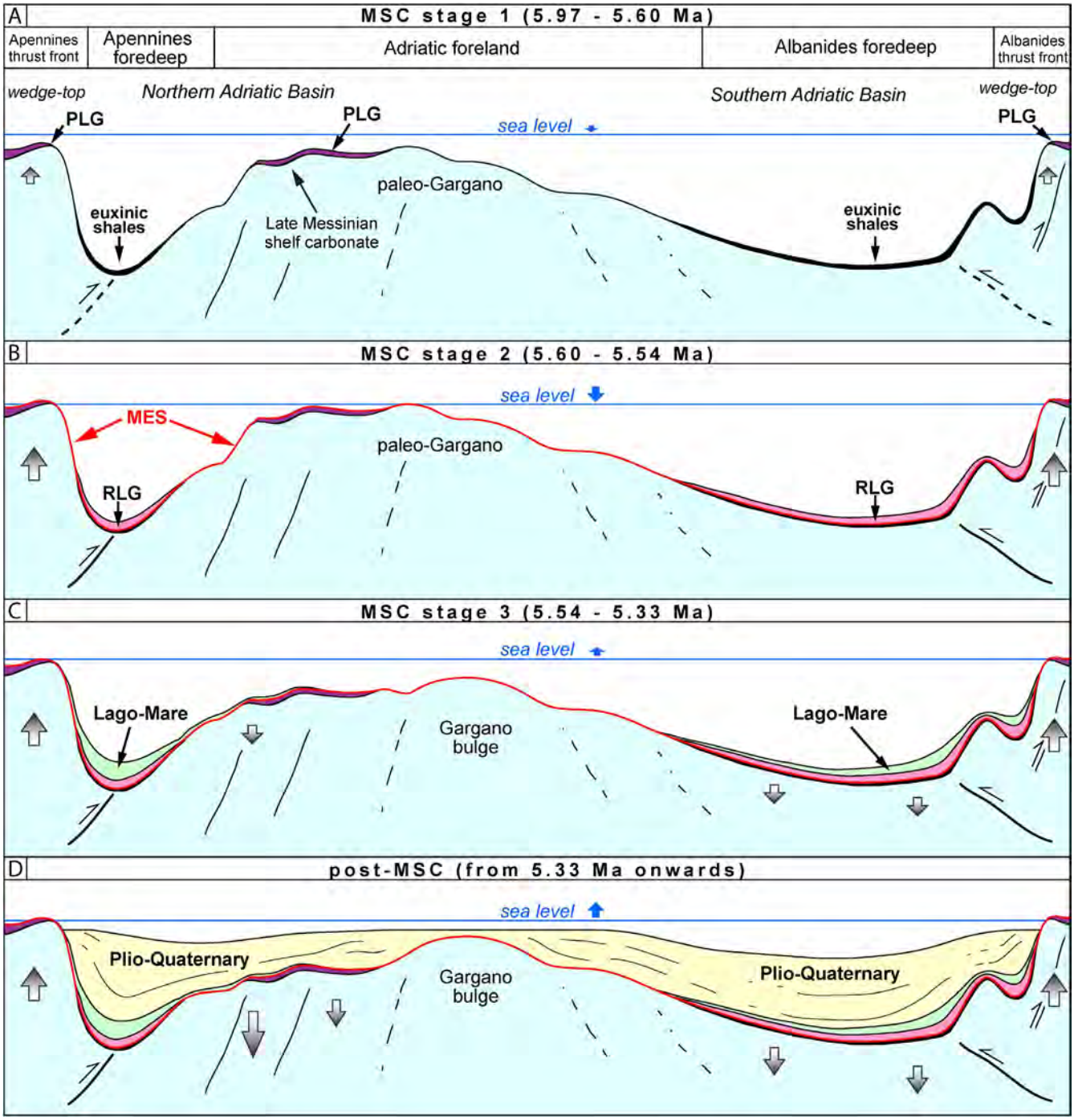


FIGURE 10 | Evolutionary pattern of the MSC in the Adriatic basin. Grey arrows = tectonic uplift and subsidence; blue arrows = eustatic fluctuations. (A) Stage1—PLG unit deposition in wedge-top settings at the front of the two orogenic ranges (Apennines and Albanian) and in the Adriatic foreland. Simultaneous deposition of euxinic shales (FBI) in foredeep contexts. (B) Stage 2—Erosion of PLG unit and accumulation of the RLG unit in the foredeep. (C) Stage 3—Deposition of Lago-mare deposits mainly in deep settings. Subsidence of the foreland ramp due to increasing lithostatic load related to westward migration of the Apennine chain. (D) End of the MSC—The return to marine conditions with deposition of Plio-Quaternary sediments. Wedge-top PLGs are exhumed onshore, while foreland PLGs remain buried offshore.

A highly debated topic, with important implications for the final stage of the crisis, concerns the halite deposition and the associated sea-level drop, which represents a cornerstone of the deep-desiccation model (Hsü et al. 1973). Estimates of the magnitude of the sea-level drawdown have changed through time (see discussion in Roveri, Lugli, et al. 2014; Roveri et al. 2025). Recently, chlorine isotopes modelling (Aloisi et al. 2024) suggested that halite precipitation occurred after a sea-level drop of about 0.85 km.

It is worth noting that the primary halite facies are only known from the Caltanissetta basin (Sicily), where the shallower portions were almost completely filled by salt. In this basin, a short-lived subaerial exposure formed within the halite unit and was

rapidly buried by the overlying deposits due to strong subsidence, suggesting that the hypothesis of a very large sea-level drop is unlikely. Moreover, the facies analysis of the deep evaporites (Hardie and Lowenstein 2004; Lugli et al. 2013, 2015) excluded the presence of shallow water to supratidal deposits that were used to justify the original desiccation model. From this perspective, the Albanian record does not provide evidence of significant exposure capable of supporting major sea-level fluctuations.

5.4.3 | The End of the Salinity Crisis

Another highly debated topic concerns the final stage of the crisis, particularly the so-called Lago-mare event (Andreetto et al. 2021, 2022) and the supposed catastrophic return of the oceanic waters into a desiccated Mediterranean at the base of the Zanclean (Garcia-Castellanos et al. 2025; Micallef et al. 2024). A comprehensive review of this topic has recently been provided by Roveri et al. (2026); to which the reader is referred for further details.

Nevertheless, the Albanian record of the third stage of the crisis shows strong similarities with coeval records in the Norther Apennines, Cyprus and Spain in terms of (i) cyclo- and physical-stratigraphic organisation, characterised by a backstepping architecture and the absence of erosional feature at the base of the Pliocene, (ii) hypohaline faunal assemblages, including the typical paratethian assemblages and (iii) isotopic signature, consistent with the typical stage 3 signal. As discussed by Roveri et al. (2026), these observations are difficult to reconcile with the existence of multiple perched and disconnected basins during the final stage of the crisis, and instead support a scenario characterised by relative high sea level allowing interconnections among the different Mediterranean sub-basins.

6 | Conclusions

The integration of onshore and offshore data allows the reconstruction of an Apennines-Albanides evolutionary model (Figure 10) matching the 3 stages evolutionary model proposed for the Messinian salinity crisis chronostratigraphy (CIESM 2008; Roveri, Lugli, et al. 2014).

During the first phase, similarly to what occurred in the Northern Apennines, the PLG unit was deposited in the marginal basins of the peri-Adriatic depression, Rubjekë (Durres) and Guri i Cifutit (Vlora) sections, and in the Adriatic foreland and backbulge basins (Manzi et al. 2020). In the Currilla (Durres coast) and Kavaje (Bigi et al. 2024) sections the stage 1 is instead expressed by an evaporite-free unit made of euxinic shales which also occurs throughout the Southern Adriatic basin and that can be interpreted as a deep-water equivalent of the PLG unit (Manzi et al. 2007); in the Kavaje section, the MSC onset (5971 Ma; Manzi et al. 2013) has been identified in this shale interval (Bigi et al. 2024).

The PLG unit, like in the Apennine foredeep basin, is truncated on top by an erosional surface. This surface, that we interpret as corresponding to the Messinian erosional surface (MES), can be traced in the deeper portions of the basin at the base of the clastic evaporites (RLG) observed in the Kavaje and Currilla sections. These deposits derived from the dismantlement of the PLG unit, as suggested by the similar isotopic strontium signature. Due to the presence of turbidite facies, thin shale intercalations, and fine gypsarenite, the Currilla section represents the deepest outcropping MSC succession. The distribution of the RLG unit can be traced in the south Adriatic basin up to the anticlines intercepted by Sparviero 001-001bis boreholes (Figure 9A).

Finally, the terrigenous succession of the Durres area (Currilla section), characterised by coarse-grained deposits reflecting an increase of continental sediment input and containing the typical faunal assemblage of the Lago-mare, can be correlated with the stage 3 deposits. Similarly to what is observed in the northern-central Apennines (Roveri et al. 1998, 2003, 2005, 2008b), these deposits pass upward to a marly unit of Zanclean age marking the return to marine conditions and the end of the salinity crisis.

Acknowledgements

This paper is dedicated to Prof. Pandeli Pashko, whose boundless enthusiasm and passion for geology inspired and made this work possible. This work has benefited from the equipment and framework of the COMP-HUB and COMP-R Initiatives, funded by the 'Departments of Excellence' program of the Italian Ministry for University and Research (MIUR, 2018–2022 and MUR, 2023–2027). Open access publishing facilitated by Universita degli Studi di Parma, as part of the Wiley - CRUI-CARE agreement.

Funding

The authors have nothing to report.

Conflicts of Interest

The authors declare no conflicts of interest.

Data Availability Statement

The data that support the findings of this study are available on request from the corresponding author. The data are not publicly available due to privacy or ethical restrictions.

References

Aloisi, G., J. Moneron, L. Guibourdenche, et al. 2024. "Chlorine Isotopes Constrain a Major Drawdown of the Mediterranean Sea During the Messinian Salinity Crisis." *Nature Communications* 15: 9671.

Andreetto, F., G. Aloisi, F. Raad, et al. 2021. "Freshening of the Mediterranean Salt Giant: Controversies and Certainties Around the Terminal (Upper Gypsum and Lago-Mare) Phases of the Messinian Salinity Crisis." *Earth-Science Reviews* 216: 103577.

Andreetto, F., R. Flecker, G. Aloisi, et al. 2022. "High-Amplitude Water-Level Fluctuations at the End of the Mediterranean Messinian Salinity Crisis: Implications for Gypsum Formation, Connectivity and Global Climate." *Earth and Planetary Science Letters* 595: 117767.

Argentino, C., F. Lugli, A. Cipriani, and G. Panieri. 2021. "Testing Miniaturized Extraction Chromatography Protocols for Combined $^{87}Sr/^{86}Sr$ and $\delta^{88}/^{86}Sr$ Analyses of Pore Water by MC-ICP-MS." *Limnology and Oceanography: Methods* 19, no. 6: 431–440.

Argnani, A. 2013. "The Influence of Mesozoic Palaeogeography on the Variations in Structural Style Along the Front of the Albanide Thrust-and-Fold Belt." *Italian Journal of Geosciences* 132: 175–185.

Argnani, A., C. Bonazzi, D. Evangelisti, et al. 1996. "Tettonica Dell'Adriatico Meridionale." *Memorie Della Societa Geologica Italiana* 51: 227–237.

Attia, O. E., E. el Khoriby, and M. A. Aref. 2004. "Sedimentology and Fluid Inclusions Criteria of the Upper Miocene (Messinian?) Gypsum Deposits in the Mediterranean Coast of Egypt." *Sedimentology (Egypt)* 12: 23–39.

Bassetti, M. A., V. Manzi, S. Lugli, et al. 2004. "Paleoenvironmental Significance of Messinian Post-Evaporitic Lacustrine Carbonates in the Northern Apennines, Italy." *Sedimentary Geology* 172: 1–18.

Bassetti, M. A., P. Miculam, and F. Ricci Lucchi. 2003. "Ostracod Faunas and Brackish-Water Environments of the Late Messinian Sapigno Section (Northern Apennines, Italy)." *Palaeo3* 198: 335–352.

Bigi, D., S. Lugli, V. Manzi, and M. Roveri. 2022. "Are Fluid Inclusions in Gypsum Reliable Paleoenvironmental Indicators? An Assessment of the Evidence From the Messinian Evaporites." *Geology* 50, no. 4: 454–459.

Bigi, D., S. Lugli, V. Manzi, et al. 2024. "The Messinian Salinity Crisis Onset in Albania: An Integrated Approach by Bio-Magnetostratigraphy and Rock Magnetic Analyses." *Palaeogeography, Palaeoclimatology, Palaeoecology* 638: 112036.

Buli, K., S. Prillo, N. Buli, L. Rumati, and R. Roqi. 2001. "Messinian Biostratigraphy Based on Foraminifers and Ostracods in Ionian Zone of Albania." *Bulletin of the Geological Society of Greece* 34, no. 2: 613–618.

CIESM. 2008. "The Messinian Salinity Crisis From Mega-Deposits to Microbiology." In *A Consensus Report, in 33eme CIESM Workshop Monographs*, edited by F. Briand, vol. 33, 1–168. CIESM.

Corcagnani, A. 2017. *La Crisi di Salinità Del Messiniano Nell'avampaese Adriatico: Ricostruzione Delle Relazioni Tra Successioni Onshore e Offshore Attraverso lo Studio di Log di Pozzo e Sismica Industriale (Database ViDEPI)*. Msc Thesis Parma University.

Cosentino, D., V. Bracone, C. D'Amico, et al. 2018. "The Record of the Messinian Salinity Crisis in Mobile Belts: Insights From the Molise Allochthonous Units (Southern Apennines, Italy)." *Palaeogeography Palaeoclimatology Palaeoecology* 503: 112–130.

Costanzo, A., M. Cipriani, M. Feely, G. Cianfione, and R. Dominici. 2019. "Messinian Twinned Selenite From the Catanzaro Trough, Calabria, Southern Italy: Field, Petrographic and Fluid Inclusion Perspectives." *Carbonates and Evaporites* 34: 743–756.

Dabrio, C. J., and M. D. Polo. 1995. "Oscilaciones Eustaticas de Alta Frequencia en el Neogeno Superior de Sorbas (Almeria, Sureste de Espana)." *Geogaceta* 18: 75–78.

de Lange, G. J., and W. Krijgsman. 2010. "Messinian Salinity Crisis: A Novel Unifying Shallow Gypsum/Deep Dolomite Formation Mechanism." *Marine Geology* 275: 273–277.

dela Pierre, F., E. Bernardi, S. Cavagna, et al. 2011. "The Record of the Messinian M. Roveri Et al./Marine Geology 352 (2014) 25–58 53 Salinity Crisis in the Tertiary Piedmont Basin (NW Italy): The Alba Section Revisited." *Palaeo3* 310: 238–255.

di Stefano, A., M. Verducci, F. Lirer, et al. 2010. "Paleoenvironmental Conditions Preceding the Messinian Salinity Crisis in the Central Mediterranean: Integrated Data From the Upper Miocene Trave Section (Italy)." *Palaeogeography, Palaeoclimatology, Palaeoecology* 297, no. 1: 37–53. https://doi.org/10.1016/j.palaeo.2010.07.012.

Evans, N. P., A. V. Turchyn, F. Gázquez, T. R. Bontognali, H. J. Chapman, and D. A. Hodell. 2015. "Coupled Measurements of δ18O and δD of Hydration Water and Salinity of Fluid Inclusions in Gypsum From the Messinian Yesares Member, Sorbas Basin (SE Spain)." *Earth and Planetary Science Letters* 430: 499–510.

Flecker, R., S. de Villiers, and R. M. Ellam. 2002. "Modelling the Effect of Evaporation on the Salinity–87Sr/86Sr Relationship in Modern and Ancient Marginal-Marine Systems: The Mediterranean Messinian Salinity Crisis." *Earth and Planetary Science Letters* 203: 221–233.

Flecker, R., and R. M. Ellam. 2006. "Identifying Late Miocene Episodes of Connection and Isolation in the Mediterranean–Paratethyan Realm Using Sr Isotopes." *Sedimentary Geology* 188: 189–203.

Fortuin, A. R., and W. Krijgsman. 2003. "The Messinian of the Nijar Basin (SE Spain): Sedimentation, Depositional Environments and Paleogeographic Evolution." *Sedimentary Geology* 160: 213–242.

Garcia-Castellanos, D., H. Heida, D. Palcu, V. Aloisi, F. Bulian, and F. Sierro. 2025. "Lagomare Kilometric Sea Level Changes During the Messinian Salinity Crisis Caused by River Erosion and Climate." *Science Advances* 11: eads9752.

García-Veigas, J., D. I. Cendón, L. Gibert, T. K. Lowenstein, and D. Artiaga. 2018. "Geochemical Indicators in Western Mediterranean Messinian Evaporites: Implications for the Salinity Crisis." *Marine Geology* 403: 197–214.

Gázquez, F., N. P. Evans, T. K. Bauska, et al. 2026. "Orbital and Eustatic Control of Basin Hydrology During the First Stage of the Messinian Salinity Crisis." *Depositional Record* 12: e70045.

Gennari, R., V. Manzi, L. Angeletti, et al. 2013. "A Shallow Water Record of the Onset of the Messinian Salinity Crisis in the Adriatic Foredeep (Legnagnone Section, Northern Apennines)." *Palaeogeography, Palaeoclimatology, Palaeoecology* 386: 145–164.

Gignoux, M. 1936. *Géologie Stratigraphique*. Masson.

Gladstone, R., R. Flecker, P. Valdes, D. Lunt, and P. Markwick. 2007. "The Mediterranean Hydrologic Budget From a Late Miocene Global Climate Simulation." *Palaeogeography, Palaeoclimatology, Palaeoecology* 251: 254–267.

Gliozzi, E. 1999. "A Late Messinian Brackish Water Ostracod Fauna of Paratethyan Aspect From Le Vicenne Basin (Abruzzi, Central Apennines, Italy)." *Palaeogeography, Palaeoclimatology, Palaeoecology* 151: 191–208.

Hardie, L. A., and T. K. Lowenstein. 2004. "Did the Mediterranean Sea Dry Out During the Miocene? A Reassessment of the Evaporite Evidence From DSDP Legs 13 and 42A Cores." *Journal of Sedimentary Research* 74: 453–461.

Hsü, K., W. B. F. Ryan, and M. Cita. 1973. "Late Miocene Desiccation of the Mediterranean." *Nature* 242: 240.

Hüsing, S. K., F. J. Hilgen, H. Abdul Aziz, and W. Krijgsman. 2007. "Completing the Neogene Geological Time Scale Between 8.5 and 12.5 ma." *Earth and Planetary Science Letters* 253: 340–358.

Hüsing, S. K., K. F. Kuiper, W. Link, F. J. Hilgen, and W. Krijgsman. 2009. "The Upper Tortonian–Lower Messinian at Monte Dei Corvi (Northern Apennines, Italy): Completing a Mediterranean Reference Section for the Tortonian Stage." *Earth and Planetary Science Letters* 282, no. 1–4: 140–157. https://doi.org/10.1016/j.epsl.2009.03.010.

Iaccarino, S., and G. Papani. 1980. *Il Messiniano Dell'Appennino Settentrionale Dalla Val d'Arda Alla Val Secchia: Stratigrafia e Rapporti col Substrato e il Pliocene*, 15–46. Universit'a Degli Studi di Parma, Volume Dedicato a Sergio Venzo. Grafiche Step Edizioni.

Iaccarino, S., and G. Salvatorini. 1982. "A Framework of Planktonic Foraminiferal Biostratigraphy for Early Miocene to Late Pliocene Mediterranean Area." *Paleontologia Stratigrafica Ed Evoluzione* 2: 115–125.

Iaccarino, S. M., A. Bertini, A. di Stefano, et al. 2008. "The Trave Section (Monte Dei Corvi, Ancona, Central Italy): An Integrated Paleontological Study of the Messinian Deposits." *Stratigraphy* 5: 281–306.

Kiratzi, A. A., and C. B. Papazachos. 1995. "Active Crustal Deformation From the Azores Triple Junction to the Middle East." *Tectonophysics* 243: 1–24.

Krijgsman, W., A. R. Fortuin, F. J. Hilgen, and F. J. Sierro. 2001. "Astrochronology for the Messinian Sorbas Basin (SE Spain) and Orbital (Precessional) Forcing for Evaporite Cyclicity." *Sedimentary Geology* 140: 43–60.

Lirer, F., L. M. Foresi, S. M. Iaccarino, et al. 2019. "Mediterranean Neogene Planktonic Foraminifer Biozonation and Biochronology." *Earth-Science Reviews* 196: 102869. https://doi.org/10.1016/j.earscirev.2019.05.013.

Longinelli, A. 1979. "Isotope Geochemistry of Some Messinian Evaporites: Paleoenvironmental Implications." *Palaeogeography, Palaeoclimatology, Palaeoecology* 29: 95–124.

Lugli, S., R. Gennari, Z. Gvirtzman, V. Manzi, M. Roveri, and B. C. Schreiber. 2013. "Evidence of Clastic Evaporites in the Canyons of the Levant Basin (Israel): Implications for the Messinian Salinity Crisis." *Journal of Sedimentary Research* 83: 942–954.

Lugli, S., V. Manzi, M. Roveri, and B. C. Schreiber. 2010. "The Primary Lower Gypsum in the Mediterranean: A New Facies Interpretation for the First Stage of the Messinian Salinity Crisis." *Palaeogeography, Palaeoclimatology, Palaeoecology* 297: 83–99.

Lugli, S., V. Manzi, M. Roveri, and B. C. Schreiber. 2015. "The Deep Record of the Messinian Salinity Crisis: Evidence of a Non-Desiccated Mediterranean Sea." *Palaeogeography, Palaeoclimatology, Palaeoecology* 433: 201–218.

Manzi, V., A. Argnani, A. Corcagnani, S. Lugli, and M. Roveri. 2020. "The Messinian Salinity Crisis in the Adriatic Foredeep: Evolution of the Largest Evaporitic Marginal Basin in the Mediterranean." *Marine and Petroleum Geology* 115: 104288. https://doi.org/10.1016/j.marpetgeo.2020.104288.

Manzi, V., R. Gennari, F. Hilgen, et al. 2013. "Age Refinement of the Messinian Salinity Crisis Onset in the Mediterranean." *Terra Nova* 25: 315–322. https://doi.org/10.1111/ter.12038.

Manzi, V., R. Gennari, S. Lugli, et al. 2018. "The Onset of the Messinian Salinity Crisis in the Deep Eastern Mediterranean Basin." *Terra Nova* 30: 189–198.

Manzi, V., R. Gennari, S. Lugli, et al. 2021. "Synchronous Onset of the Messinian Salinity Crisis 1 and Diachronous Evaporite Deposition: New Evidences From the Deep Eastern Mediterranean Basin." *Palaeogeography, Palaeoclimatology, Palaeoecology* 584: 110685.

Manzi, V., S. Lugli, F. Ricci Lucchi, and M. Roveri. 2005. "Deep-Water Clastic Evaporites Deposition in the Messinian Adriatic Foredeep (Northern Apennines, Italy): Did the Mediterranean Ever Dry Out?" *Sedimentology* 52: 875–902.

Manzi, V., M. Roveri, R. Gennari, et al. 2007. "The Deep-Water Counterpart of the Messinian Lower Evaporites in the Apennine Foredeep: The Fanantello Section (Northern Apennines, Italy)." *Palaeogeography, Palaeoclimatology, Palaeoecology* 251: 470–499.

Matano, F., M. Barbieri, S. di Nocera, and M. Torre. 2005. "Stratigraphy and Strontium Geochemistry of Messinian Evaporite-Bearing Successions of the Southern Apennines Foredeep, Italy: Implications for the Mediterranean "Salinity Crisis" and Regional Palaeogeography." *Palaeogeography, Palaeoclimatology, Palaeoecology* 217: 87–114.

McArthur, J. M. 1994. "Recent Trends in Strontium Isotope Stratigraphy." *Terra Nova* 6: 331–358.

McArthur, J. M., R. J. Howarth, and T. R. Bailey. 2001. "Strontium Isotope Stratigraphy: LOWESS Version 3: Best Fit to the Marine Sr-Isotope Curve for 0-509 ma and Accompanying Look-Up Table for Deriving Numerical Age." *Journal of Geology* 109: 155–170.

Micallef, A., G. Barraca, C. Hubscher, et al. 2024. "Land-To-Sea Indicators of the Zanclean Megaflood." *Communications Earth & Environment* 5: 794.

Muço, B. 1994. "Focal Mechanism Solutions for Albanian Earthquakes for the Years 1964–1988." *Tectonophysics* 231: 311–323.

Natalicchio, M., F. dela Pierre, S. Lugli, et al. 2014. "Did Late Miocene (Messinian) Gypsum Precipitate From Evaporated Marine Brines? Insights From the Piedmont Basin (Italy)." *Geology* 42: 179–182. https://doi.org/10.1130/G34986.1.

Natalicchio, M., L. Pellegrino, P. Clari, L. Pastero, and F. dela Pierre. 2021. "Gypsum Lithofacies and Stratigraphic Architecture of a Messinian Marginal Basin (Piedmont Basin, NW Italy)." *Sedimentary Geology* 425: 106009.

Omodeo-Sale', S., R. Gennari, S. Lugli, V. Manzi, and M. Roveri. 2012. "Tectonic and Climatic Control on the Late Messinian Sedimentary Evolution of theNijar Basin (Betic Cordillera, Southern Spain)." *Basin Research* 24: 314–337.

Ori, G. G., M. Roveri, and F. Vannoni. 1986. "Plio-Pleistocene Sedimentaton in the Apenninic Adriatic Foredeep (Central Adriatic Sea, Italy)." In *Foreland Basin*, edited by P. A. Allen and P. Homewood, vol. 8, 183–198. Spec. Pub. Int. Ass. Sed.

Orszag-Sperber, F. 2006. "Changing Perspectives in the Concept of "Lago-Mare" in Mediterranean Late Miocene Evolution." *Sedimentary Geology* 188–189: 259–277.

Panieri, G., S. Lugli, V. Manzi, M. Roveri, B. C. Schreiber, and K. A. Palinska. 2010. "Ribosomal RNA Gene Fragments From Fossilized Cyanobacteria Identified in Primary Gypsum From the Late Miocene, Italy." *Geobiology* 8: 101–111.

Pashko, P. 1973. "Messiniani ne Zonen Jonike." *Permbl. Srudimesh* 3: 51–69.

Pashko, P., I. Milushi, and V. Hoxha. 2017. The Messinian Evaporites of the Periadriatic Foreland Basin (Albania).

Pashko, S., and S. Aliaj. 2020. "Stratigraphy and Tectonic Evolution of Late Miocene - Quaternary Basins in Eastern Albania: A Review." *Bulletin of the Geological Society of Greece* 56, no. 1: 317–351. https://doi.org/10.12681/bgsg.22064.

Pondrelli, S., A. Morelli, and E. Boschi. 1995. "Seismic Deformation in the Mediterranean Area Estimated by Moment Tensor Summation." *Geophysical Journal International* 122: 938–952.

Prillo, S., and L. Hasanaj. 2002. "Biostratigraphy and Paleoenviroments of the Late Messinian Sediments of the Durr¨es-Lushnja Area, Albania." In *Bulletin T. CXXV de l'Academie Serbe Des Sciences et Des Arts*. Classe des Sciences Mathbnatiques et Fzaturelles Sciences Naturelles 41.

Reghizzi, M., S. Lugli, V. Manzi, F. P. Rossi, and M. Roveri. 2018. "Orbitally Forced Hydro-Logical Balance During the Messinian Salinity Crisis: Insights From Strontium Iso-Topes (87Sr/86Sr) in the Vena Del Gesso Basin (Northern Apennines, Italy)." *Paleoceanography and Paleoclimatology* 33: 716–731. https://doi.org/10.1029/2018PA003395.

Ricchetti, G., N. Ciaranfi, E. Luperto Sinni, F. Mongelli, and P. Pieri. 1988. "Geodinamica ed Evoluzione Sedimentaria e Tettonica Dell'Avampaese Apulo." *Memorie Della Societa Geologica Italiana* 41: 57–82.

Roep, T. B., C. J. Dabrio, A. R. Fortuin, and M. D. Polo. 1998. "Late Highstand Patterns of Shifting and Stepping Coastal Barriers and Washover-Fans (Late Messinian, Sorbas Basin, ES Spain)." *Sedimentary Geology* 116: 27–56.

Rossi, M., M. Minervini, M. Ghielmi, and S. Rogledi. 2015. Messinian and Pliocene Erosional Surfaces in the Po Plain-Adriatic Basin: Insights From Allostratigraphy and Sequence Stratigraphy in Assessing Play Concepts Related to Accommodation and Gateway Turnarounds in Tectonically Active Margins.

Rouchy, J. M., and A. Caruso. 2006. "The Messinian Salinity Crisis in the Mediterranean Basin: A Reassessment of the Data and an Integrated Scenario." *Sedimentary Geology* 188: 35–67.

Roveri, M., M. A. Bassetti, and F. Ricci Lucchi. 2001. "The Mediterranean Messinian Salinity Crisis: An Apennine Foredeep Perspective." *Sedimentary Geology* 140: 201–214.

Roveri, M., A. Boscolo Gallo, M. Rossi, et al. 2005. "The Adriatic Foreland Record of Messinian Events (Central Adriatic Sea, Italy)." *GeoActa* 4, no. 139: 158.

Roveri, M., A. Cipriani, R. Gennari, S. Lugli, V. Manzi, and M. Taviani. 2026. "Lago-Mare - A New Scenario for the Final Stage and the End of the Messinian Salinity Crisis." *Earth-Science Reviews* 274: 105380.

Roveri, M., R. Flecker, W. Krijgsman, et al. 2014. "The Messinian Salinity Crisis: Past and Future of a Great Challenge for Marine Sciences." *Marine Geology* 352: 25–58.

Roveri, M., R. Gennari, S. Lugli, and V. Manzi. 2009. "The Terminal Carbonate Complex: The Record of Sea-Level Changes During the Messinian Salinity Crisis." *GeoActa* 8: 57–71.

Roveri, M., S. Lugli, V. Manzi, et al. 2006. "The Record of Messinian Events in the Northern Apennines Foredeep Basins." *Acta Naturalia de L'ateneo Parmense* 42: 47–123.

Roveri, M., S. Lugli, and V. Manzi. 2025. "The Desiccation and Catastrophic Refilling of the Mediterranean: 50 Years of Facts, Hypotheses, and Myths Around the Messinian Salinity Crisis." *Annual Review of Marine Science* 17: 485–509.

Roveri, M., S. Lugli, V. Manzi, R. Gennari, and B. C. Schreiber. 2014. "High-Resolution Strontium Isotope Stratigraphy of the Messinian Deep Mediterranean Basins: Implications for Marginal to Central Basins Correlation." *Marine Geology* 349: 113–125.

Roveri, M., S. Lugli, V. Manzi, M. Reghizzi, and F. P. Rossi. 2020. "Stratigraphic Relationships Between Shallow-Water Carbonates and Primary Gypsum: Insights From the Messinian Succession of the Sorbas Basin (Betic Cordillera, Southern Spain)." *Sedimentary Geology* 404: 105678.

Roveri, M., S. Lugli, V. Manzi, and B. C. Schreiber. 2008a. "The Messinian Sicilian Stratigraphy Revisited: Toward a New Scenario for the Messinian Salinity Crisis." *Terra Nova* 20: 483–488.

Roveri, M., S. Lugli, V. Manzi, and B. C. Schreiber. 2008b. *The Messinian Salinity Crisis: A Sequence- Stratigraphic Approach*. Vol. 1, 169–190. GeoActa Special Publ.

Roveri, M., V. Manzi, M. A. Bassetti, M. Merini, and F. Ricci Lucchi. 1998. "Stratigraphy of the Messinian Post-Evaporitic Stage in Eastern-Romagna (Northern Apennines, Italy)." *Giornale di Geologia* 60: 119–142.

Roveri, M., V. Manzi, F. Ricci Lucchi, and S. Rogledi. 2003. "Sedimentary and Tectonic Evolution of the Vena Del Gesso Basin (Northern Apennines, Italy): Implications for the Onset of the Messinian Salinity Crisis." *Geological Society of America Bulletin* 115: 387–405.

Ruggieri, G. 1967. "The Miocene and Later Evolution of the Mediterranean Sea." In *Aspects of Tethyan Biogeography, 7*, edited by C. G. Adams and A. V. Ager, 283–290. Systematics Association Publ.

Ryan, W. B. F., and F. Raad. 2025. "Introducing a Water Activity Coefficient to Account for Abundance and Isotopic Compositions of Gypsum and Halite in the Mediterranean's Salt Giant Deposit." *Sedimentary Geology* 481: 197–214.

Selli, R. 1952. *Su un Livello Guida Nel Messiniano Romagnolo-Marchigiano*, 192–195. Atti VII Convegno Nazionale Del Metano, Taormina.

Selli, R. 1954. "Il Bacino Del Metauro." *Giornale di Geologia* 24: 1–294.

Sextos, A., E. Lekkas, S. Stefanidou, et al. 2020. "ETAM Report on the Albania Earthquake of November 26, 2019. In: Structural and Geotechnical Damage." https://doi.org/10.13140/RG.2.2.16153.24167.

Shërbimi Gjeologjik Shqiptar. 2002. Harta Gjeologjike e Shqip¨Eris¨e Shkalla 1:200 000.

Topper, R. P. M., R. Flecker, P. T. Meijer, and M. J. R. Wortel. 2011. "A Box Model of the Late Miocene Mediterranean Sea: Implications From Combined 87Sr/86Sr and Salinity Data." *Paleoceanography* 26: PA3223.

Topper, R. P. M., S. Lugli, V. Manzi, M. Roveri, and P. T. Meijer. 2014. "Precessional Control of Sr Ratios in Marginal Basins During the Messinian Salinity Crisis?" *Geochemistry, Geophysics, Geosystems* 15: 1926–1944. https://doi.org/10.1002/2013GC005192.

Topper, R. P. M., and P. T. Meijer. 2013. "A Modelling Perspective on Spatial and Temporal Variations in Messinian Evaporite Deposits." *Marine Geology* 336: 44–60.

van Couvering, J. A., D. Castradori, M. B. Cita, F. J. Hilgen, and D. Rio. 2000. "The Base of the Zanclean Stage and of the Pliocene Series." *Episodes* 23: 179–187.

Vannucci, G., S. Pondrelli, A. Argnani, A. Morelli, P. Gasperini, and E. Boschi. 2004. "An Atlas of Mediterranean Seismicity." *Annali di Geofisica* 47: 247–306.

Xhomo, A., A. Kodra, K. Gjata, and Z. Xhafa. 1999. *Geotectonic Map of Albania, Scale 1:200000*. Geological Survey of Albania.

Supporting Information

Additional supporting information can be found online in the Supporting Information section. **Table S1:** List of samples used for petrographic analysis on transmitted light microscope. Twenty-nine standard thin sections of evaporite, carbonate and terrigenous rocks were studied with transmitted light. Among these, 15 come from the Guri i Cifutit (Vlore) section and 11 from the Currilla section (Durres coast) and 1 Rubjeke section (Preze monocline). **Table S2:** List of samples used for biostratigraphic analysis. A total of 37 samples were analysed, 10 of which from the Vlora area and 27 from the Durres area. Samples were washed through a 63 μm mesh sieve and the fraction > 125 μm was used to perform qualitative analyses. **Table S3:** List of samples used for geochemical isotopic analysis. Ten samples from evaporites and from hypohaline mollusc assemblages have been analysed for $^{87}Sr/^{86}Sr$.